Simulations of Mesoscale Convective Systems

Wei-Kuo Tao, Joanne Simpson and Brad Ferrier
Mesoscale Atmospheric Processes Branch (Code 912)
Laboratory for Atmospheres
NASA/Goddard Space Flight Center
Greenbelt, MD 20771

Abstract: In this paper, we will present the results obtained from cloud resolving model (CRM) simulations. Three specific topics will be discussed. **(1)** Differences as well as similarities in terms of heating and moisture budgets as well as cloud-radiation interactive processes between two types of modeled convection systems (large-scale continuously forced and self-forced convection) will be discussed. **(2)** We will identify the main physical processes which can produce very different "*statistical-equilibrium temperature and water vapor fields*". **(3)** We will present results from CRMs that can be used to understand and to improve the cumulus parameterization closure assumptions as well as to show the interaction with explicit microphysics.

1. Introduction

The hydrological cycle distinguishes the Earth from the other planets. A key link in the hydrological cycle is the rain which falls from cloud systems in the tropics, which amounts to about two-thirds of the global precipitation. Precipitation, by means of its associated latent heat release, is the major energy source driving the hydrological cycle and the large-scale circulation of the atmosphere. Recently studies pointed out that the primary reason for differences in current climate model simulations is the treatment of cloud-radiation interaction processes. Clearly, if the prediction of the global/regional climate change is to be reliable, the effects of clouds (microphysical processes) must be accurately represented in climate models. An international program, the GEWEX Cloud System Study (GCSS), was initiated to improve the representation of cloud processes in climate and NWP models. The GCSS Science Team (1993) recommended that improved cloud-resolving models (CRMs) or cumulus ensemble models should be used as a test bed to develop and evaluate the cloud parameterization for large-scale models.

Cloud resolving (or cumulus ensemble) models (CRMs) are, perhaps, one of the most important tools used to establish quantitative relationships between diabatic heating and rainfall. This is because latent heating is dominated by phase changes between water vapor and small, cloud-sized particles, which can not be directly detected (though some passive microwave frequencies do respond to path-integrated cloud water). The CRMs, however, explicitly simulate the conversion of cloud condensate into raindrops and various forms of precipitation ice. It is

these different forms of precipitation that are most readily detected from space, and which ultimately reach the surface in the form of rain in the Tropics (Simpson and Tao, 1993; Simpson *et al.*, 1989; 1996).

The use of cloud resolving models (CRMs) in the study of tropical convection and its relation to the large-scale environment can be generally categorized into two groups. The first approach is so-called "cloud ensemble modeling". In this approach, many clouds of different sizes in various stages of their lifecycles can be present at any model simulation time. The large-scale effects which are derived from observations are imposed into the models as the main forcing, however. In addition, the cloud ensemble models use cyclic lateral boundary conditions (to avoid reflection of gravity waves) and require a large horizontal domain (to allow for the existence of an ensemble of clouds). The clouds simulated from this approach could be termed "***continuous large-scale forced convection***". On the other hand, the second type of cloud resolving models do not require large-scale effects to initialize the clouds. This type of CRM usually requires initial temperature and water vapor profiles which have a medium to large CAPE, and an open lateral boundary condition is used. The modeled clouds, then, are initialized with either a cool pool, warm bubble or surface processes (i.e., land/ocean). These modeled clouds could be termed "***self-forced convection***".

In this paper, we will present the results obtained from both approaches. **(1)** Differences as well as similarities between two modeled convection systems will be discussed. Specifically, we will present results associated with cloud-radiation interaction for both large-scale forced convection and self-forced convection. **(2)** We will identify the main physical processes which can produce very different "*statistical-equilibrium temperature and water vapor fields*". For example, Grabowski *et al.* (1996) found that the modeled climate was warm and humid in their 24 day simulation. Sui *et al.* (1994), however, simulated a cool and dry climate after 60 days of simulation. **(3)** We will present results from CRMs that can be used to improve cumulus parameterization closure assumptions (Ferrier *et al.*, 1996) as well as to show the interaction with explicit microphysics (Tao *et al.*, 1993; Tao, 1995).

2. Cloud Resolving Model (CRM)

During the past 20 years, observational data on atmospheric convection has been accumulated from measurements by various means, including radars, instrumented aircraft, satellites, and rawinsondes in special field observations (*e.g.*, GATE, PRE-STORM, COHMEX, TAMEX, EMEX and several others). This has made it possible for convective cloud modelers to test their simulations against observations, and thereby improve their models. In turn, the models have provided a necessary framework for relating the fragmentary observations and helping to understand the complex physical processes interacting in atmospheric convective systems, for which observations alone still cannot provide a dynamically consistent four-dimensional picture. The past decades have also seen substantial advances in the numerical modeling of convective clouds and mesoscale convective systems (*e.g.*, squall-type and non-squall-type convective

systems), which have substantially elucidated complex dynamical cloud-environment interactions in the presence of varying vertical wind shear. With the advent of powerful scientific computers, many important and complex processes (which require extensive computations), such as ice-microphysics and radiative transfer, can now be simulated to a useful (but still oversimplified) degree in these numerical cloud models.

The Goddard Cumulus Ensemble (GCE) model is a cloud resolving model, and its main features have been extensively published, recently by Tao and Simpson (1993) and Simpson and Tao (1993). The model is nonhydrostatic and model variables include horizontal and vertical velocities, potential temperature, perturbation pressure, turbulent kinetic energy, and mixing ratios of all water phases (vapor, liquid, and ice). The following major improvements have been made to the model during the past three-year period: **(i)** The development of an improved four-class, multiple-moment, multiple-phase ice scheme (Ferrier, 1994), which resulted in improved agreement with observed radar and hydrometeor structures for convective systems simulated in different geographic locations without the need for adjusting coefficients (Ferrier *et al.*, 1995). **(ii)** The inclusion of solar and infrared radiative transfer processes, which have been used to study the impact of radiation upon the development of clouds and precipitation (Tao *et al.*, 1993; 1996) and upon the diurnal variation of rainfall (Tao *et al.*, 1996) for tropical and midlatitude squall systems. **(iii)** The incorporation of land and ocean surface processes to investigate their impact upon the intensity and development of organized convective systems (Wang *et al.*, 1996a; Lynn and Tao, 1996). Mesoscale circulations, which formed in response to landscape heterogeneities represented by a land surface model, were crucial in the initiation and organization of the convection (Lynn*et al.*, 1996). Table 1 lists the Characteristics of the GCE model.

Parameters/Processes	GCE Model
Vertical Coordinate	z
Explicit Convective Processes	2 class water & 2 moment 4 class ice
Implicit Convective Processes	None
Numerical Methods	Positive Definite Advection for Scalar Variables; 4-th Order for Dynamic Variables
Initialization	Initial Condition with Forcing from Observations/Large-Scale Model
FDDA	None
Radiation	Broad-Band in LW; Solar Explicit Cloud-radiation Interaction
Sub-Grid Diffusion	TKE
Planetary Boundary Processes	None
Topography	Sigma-z
Two-Way Interactive Nesting	Radiative-Type
Surface Energy Budget	Force-restore Method 7-Layer Soil Model (PLACE) TOGA COARE Flux Module

Table 1 Characteristics of Goddard Cumulus Ensemble Model

3. Response of Deep Cloud Systems to Large-Scale Processes in Various Geographic Locations

3.1 Heating and Moisture Budgets

In diagnostic studies (*e.g.*, Yanai *et al.*, 1973), it is customary to define the apparent heat source Q_1 and the apparent moisture sink Q_2 of a large-scale system by averaging horizontally the thermodynamic and water vapor equations as:

$$\mathbf{Q_1} = \overline{\pi}[\frac{\partial\overline{\theta}}{\partial t} + \overline{\vec{\mathbf{V}}} \bullet \nabla\overline{\theta} + \overline{\mathbf{w}}\frac{\partial\overline{\theta}}{\partial \mathbf{z}}] - \mathbf{Q_{R'}} \tag{1}$$

$$\mathbf{Q_2} = -\frac{\mathbf{L_v}}{\mathbf{C_P}}[\frac{\partial\overline{\mathbf{q}}_\mathbf{V}}{\partial t} + \overline{\vec{\mathbf{V}}} \bullet \nabla\overline{\mathbf{q}}_\mathbf{V} + \overline{\mathbf{w}}\frac{\partial\overline{\mathbf{q}}_\mathbf{V}}{\partial \mathbf{z}}]. \tag{2}$$

Q_1 and Q_2 can be calculated either from observations or from grid values in a large- or regional-scale prediction model. Q_1 and Q_2 can directly relate to the contributions of cloud effects which can be explicitly estimated by the CRMs (Soong and Tao, 1980; Tao, 1983; Tao and Soong, 1986; Tao and Simpson, 1989b and many others):

$$\mathbf{Q_1} = \overline{\pi}[-\frac{1}{\overline{\rho}}\frac{\partial\overline{\rho}\,\overline{\mathbf{w}'\theta'}}{\partial \mathbf{z}} + \mathbf{D}_\theta] + \frac{\mathbf{L_v}}{\mathbf{C_P}}(\overline{\mathbf{c}} - \overline{\mathbf{e}}_\mathbf{c} - \overline{\mathbf{e}}_\mathbf{r}) + \frac{\mathbf{L_f}}{\mathbf{C_P}}(\overline{\mathbf{f}} - \overline{\mathbf{m}}) + \frac{\mathbf{L_s}}{\mathbf{C_P}}(\overline{\mathbf{d}} - \overline{\mathbf{s}}) + \overline{\mathbf{Q}}_{\mathbf{R'}} \tag{3}$$

$$\mathbf{Q_2} = \frac{\mathbf{L_v}}{\mathbf{C_P}}[\frac{1}{\overline{\rho}}\frac{\partial\overline{\rho}\,\overline{\mathbf{w}'\mathbf{q}'_\mathbf{V}}}{\partial \mathbf{z}} - \overline{\mathbf{D}}_{\mathbf{q_V}}] + \frac{\mathbf{L_v}}{\mathbf{C_P}}(\overline{\mathbf{c}} - \overline{\mathbf{e}}_\mathbf{c} - \overline{\mathbf{e}}_\mathbf{r}) + \frac{\mathbf{L_s}}{\mathbf{C_P}}(\overline{\mathbf{d}} - \overline{\mathbf{s}}). \tag{4}$$

The overbars denote horizontal averages, and the primes indicate deviations from the horizontal averages. The variable $\overline{\rho}$ is the density, and $\overline{\pi} = (\mathbf{p}/\mathbf{P_{oo}})^{\mathbf{R}/\mathbf{C_p}}$ is the nondimensional pressure, where $\mathbf{P}$ is the dimensional pressure and $\mathbf{P_{oo}}$ the reference pressure taken to be 1000 mb. C_p is the specific heat of dry air at constant pressure, and R is the gas constant for dry air. The variables L_v, L_f and L_s are the latent heats of condensation, fusion and sublimation, respectively. The variables c, e_c, e_r, f, m, d and s stand for the rates of condensation, evaporation of cloud droplets and raindrops, freezing of raindrops, melting of snow and graupel/hail, deposition of ice particles and sublimation of ice particles, respectively. The term $\mathbf{Q_R}$ is the cooling/heating rate associated with radiative processes. Also, the first terms on the right-hand side of (3) and (4) are the vertical eddy heat and moisture

flux convergences, respectively. The subgrid scale turbulence terms are represented by $\mathbf{D}_\theta$ and $\mathbf{D}_q$ and are negligibly small compared to the other terms (Soong and Tao, 1980; Krueger, 1988). Eqs. (3) and (4) represent the cloud heating and drying effects, respectively.

(a) Diagnostically Determined Heating and Moisture Budgets

Figure 1 shows several Q_1 profiles derived from several diagnostic studies. Figure 1 indicates clearly that the heating profiles do show marked variation among different types of cloud systems. For example, the maximum heating peaks between the 4 and 7 km levels. The heating profiles associated with each of these systems, however, share many common features after they are decomposed into their convective and stratiform components. For example, a composite of heating profiles obtained from the results of five different diagnostic studies (Yanai *et al.*, 1973; Johnson, 1984; Houze, 1989; Chong and Hauser, 1990; Gallus and Johnson, 1991) and one modeling study (Lafore and Redelsperger, 1991) are presented in Fig. 2 for both the convective and stratiform regions. They include cases from West Africa, the tropical eastern Atlantic (GATE), the west-central Pacific (Marshall Island), and the central-southern Plains of the U.S. (PRE-STORM). The spacial resolution as well as the partitioning between the convective and stratiform regions is not consistent among these diagnostic studies. The convective profiles show heating throughout the depth of the troposphere which is maximized in the lowest 2-5 km. The shapes of the heating profiles are quite similar with only slight variations in their magnititude. The same can generally be said about the stratiform region. Heating is maximized in the upper troposphere, however, between 5 and 9 km while cooling prevails at about 4 km.

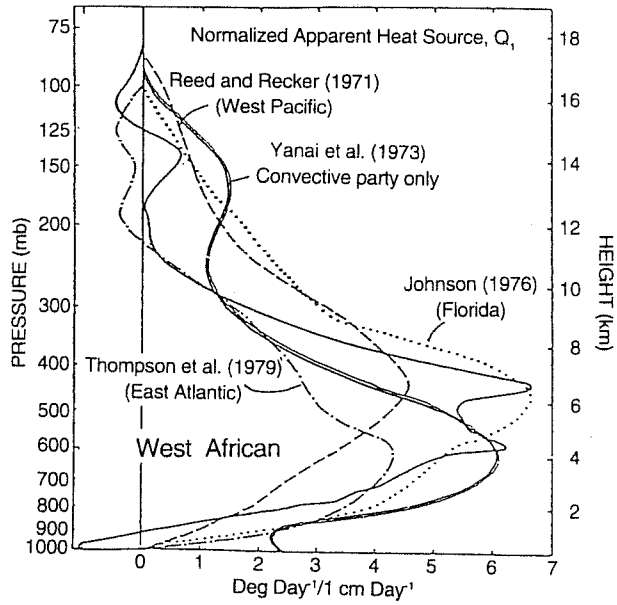

Fig. 1 Comparison of vertical Q_1 profiles normalized by rainfall rates. These profiles are from Gallus and Johnson (1991, curve GJ), Yanai et al. (1973; but was partitioned into convective and stratiform components by Johnson, 1984, curve Y), Houze, (1989, curve H), Houze and Rappaport (1984, curve HR), and Chong and Hauser (1990, curve CH).

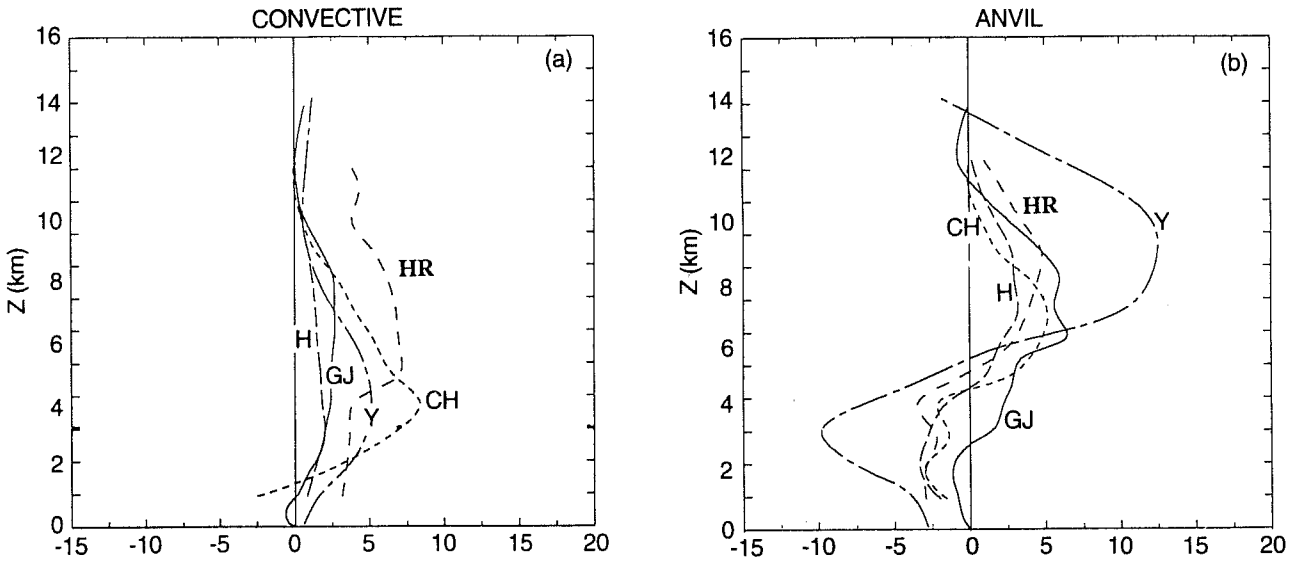

Fig. 2 Comparison of vertical Q_1 profiles normalized by rainfall rates for averages taken (a) over the convective region and (b) over the stratiform region. These profiles are from Gallus and Johnson (1991, curve GJ), Yanai et al. (1973; but was partitioned into convective and stratiform components by Johnson, 1984, curve Y), Houze, (1989, curve H), Houze and Rappaport (1984, curve HR), and Chong and Hauser (1990, curve CH). Adapted from Tao et al. (1993)

(b) CRM Simulated Heating and Moisture Budgets

Tables 2 and 3, respectively, summarize most of the previous (prior to 1994) CRMs' studies associated with continuously large-scale forced and self-forced convection. Both CRMs have the same physics with the major difference being their model setup. The CRM for simulating clouds under continuous large-scale forcing allows several convective clouds to develop simultaneously inside the model domain. A time-varying large-scale lifting and/or advective effects on temperature and water vapor with magnititudes deduced from observations is imposed continuously in the model as the main forcing mechanism. In order to randomize the development of clouds, small horizontal random disturbances are applied to the temperature (water vapor or wind) field in the model in the middle of the subcloud layer[1]. A simple periodic boundary condition is used in the horizontal. Under these conditions, a simulated cloud near one boundary may exit the domain and reenter on the other side. With an open boundary condition, a simulated cloud can propagate through the lateral boundary with minimal

1 The use of horizontal inhomogeneities in the surface fluxes of heat and moisture to initiate the cloud fields has been previously considered (Hill, 1974, 1977; Sommeria, 1976; Yau and Michaud, 1982).

backward reflection in an ideal situation, but it will generate additional uncontrolled nonzero mean vertical velocities that pass through the lateral boundaries of the domain (Clark, 1979). Such motion complicates the budget study because the total large-scale effects then realized in the model will deviate from the observations. In the CRM for simulating convective systems without continuous large-scale forcing, the convective clouds are generally initiated by a low-level cool pool and/or warm bubble. It also needs to use an environmental sounding (usually from a field campagin) with moderate to high convective available potential energy (CAPE). Open lateral boundary conditions are used. Clearly, both approaches have their own limitations based on their assumptions. The purpose of this study is to find out whether or not there are significant differences in their respectively modeled Q_1, Q_2 and momentum budgets.

	Model	Microphysics	Turbulence	Domain	Integration
Soong & Ogura (1980)	2-D	Water	Prognostic TKE	64 km	24 h
Soong & Tao (1980)	2-D	Water	Prognostic TKE	64 km	24 h
Soong & Tao (1984)	2-D	Water	Prognostic TKE	128 km	6 h
Ogura & Jiang (1985)	2-D	Water	Prognostic TKE	128 km	16 h
Tao & Soong (1986)	3-D	Water	Prognostic TKE	32 x 32 km^2	6 h
Lipps & Helmer (1986)	2-D 3-D	Water	Prognostic TKE	32-64 km 24 x 16 km^2	4 h
Tao, Simpson & Soong (1987)	2-D 3-D	Water	Prognostic TKE	128 km 32 x 32 km^2	6 h
Nikajima & Matsuno (1988)	2-D	Water	K-type	512 km	50 h
Dudhia & Moncrieff (1987)	3-D	Water	Prescribed fluxes	25 x 50 km^2	3 h
Krueger (1988)	2-D	Water	3rd Moment	30 km	2 h
Tao & Simpson (1989)	2-D 3-D	Water & Ice	Prognostic TKE	512 km 96 x 96 km^2	12 h 4 h
Gregory & Miller (1989)	2-D	Water	Prescribed fluxes	256 km	9 h
Xu & Krueger (1991)	2-D	Water & Ice	3rd moment	512 km	120 h
McCumber, Tao, Simpson, Penc & Soong (1992)	2-D 3-D	Water Water & Ice	Prognostic TKE	512 km 64 x 32 km^2	12 h 3 h
Xu, Arakawa & Krueger (1992)	2-D	Water & Ice	3rd moment	512 km	120 h
Held, Hemler & Ramaswamy (1993)	2-D	Water & Ice	K-theory	640 km	1000 h
Sui, Lau, Tao, Simpson & Chou (1993)	2-D	Water & Ice	Prognostic TKE	768 km	1248 h

Table 2 Summary of previous modeling studies of the response of cumulus clouds to continuous large-scale influences. The general setup for each study is given along with some of the model characteristics and treatments used to parameterize microphysics and turbulence.

	Model	Microphyics	Turbulence	Radiation	Domain	Integration
Nicholls (1987)	2-D	Water & Ice	Prognostic TKE	No	400 km	5 h
Rotunno, Klemp & Weisman (1988)	2-D 3-D	Water	Prognostic TKE	No	180 km 180 x 120 km^2	8 h
Lafore, Re-delsperger & Jaubert (1988)	3-D	Water	2nd Moment	No	80 x 50 km^2	8 h
Fovell & Ogura (1988)	2-D	Water & Ice	Prognostic TKE	No	4000 km Stretched	12 h
Lafore & Moncrieff (1989)	2-D	Water	K-type	No	480 km and Nested	12 h
Schlesinger (1991)	3-D	Water	K-type	No	58 x 58 km^2	1 h
Tao, Simpson & Soong (1991)	2-D	Water & Ice	Prognostic TKE	IR	666 km and Stretched	8 h
Tao , Simpson, Sui, Ferrier, Lang, Scala, Chou & Pickering (1993)	2-D	Water & Ice	Prognostic TKE	IR	1025 km Stretched	16 h

Table 3 Same as Table 2 except for self-forced convection.

The 2-D version of the CRM was first applied to shallow moist convection by Soong and Ogura (1980), and to deep convection by Soong and Tao (1980). Tao (1983) has added the third dimension and Tao and Simpson (1989b) have included ice microphysical processes in the cloud ensemble model. Figure 3(a) shows the vertical profiles of heating and cooling for a GATE convective line which was simulated by the three-dimensional model with continuous large-scale forcing (Tao and Soong, 1986). The heating due to the vertical flux of sensible heat by convective clouds, **F**, is one order of magnitude smaller than that produced by condensation at most levels. On the other hand, the maximum value of the cooling rate by evaporation, **e**, is more than half of the heating rate by condensation. This finding implies that the sum of the condensation and evaporation would provide a good approximation of the total cloud heating rate. The cloud heating effect would be considerably overestimated if heating by condensation alone is considered, ignoring cooling by evaporation. Fig. 3(b) shows the vertical profiles of moistening and drying due to the clouds. The net vertical flux of moisture by clouds is generally smaller than the rate of condensation or evaporation, but it is not negligible. The corresponding Q_1 and Q_2 profiles obtained from the large-scale variables are also shown in Fig. 3 for comparison. The model generated heating and drying effects agree well with those estimated from observations.

The GCE model without applying continuous large-scale forcing has been used to simulate a tropical oceanic (EMEX; Equatorial Mesoscale EXperiment) and a mid latitude continental squall line (PRE-STORM; Preliminary Regional Experiment for STORM central). Ice-microphysical processes and long wave

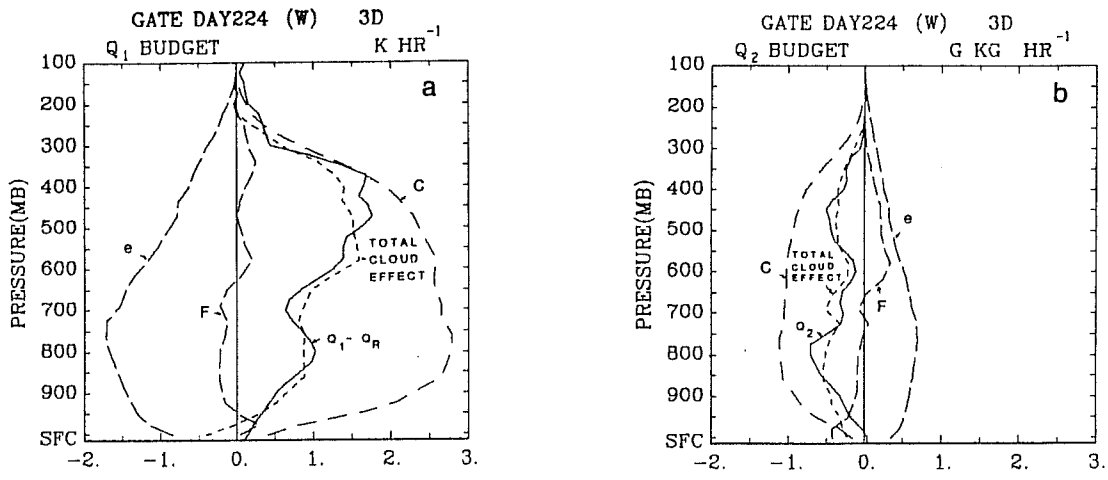

Fig. 3 ***(a)*** *Vertical profiles of heating rates by condensation of moisture,* ***c****, evaporation of liquid water drops,* ***e****, net vertical flux of sensible heat,* ***F****, the total heating rate by clouds and the heating rate estimated from large-scale observations,* $Q_1 - Q_R$. ***(b)*** *Vertical profiles of moistening rates by condensation of moisture, evaporation from liquid water drops, net vertical moisture flux, the total moistening rate by clouds and the moistening rate estimated from the large-scale observations,* $-(c_p/L)Q_2$.

radiative transfer processes are fully included in these two simulations. These two squall lines developed in quite different environments (see Fig. 1 in Tao *et al.*, 1993). For example, the CAPE (Convective Available Potential Energy) for the EMEX squall line is much smaller (1484 m^2 s^{-2}) than that of the PRE-STORM case (2300 m^2 s^{-2}). Also, the vertically integrated water vapor contents are quite different, specifically 6.175 and 4.385 g g^{-1} cm^{-2} for the EMEX and PRE-STORM cases, respectively. A very moist environment in the western Pacific region (WMONEX, AMEX) is quite common. The simulated squall systems captured several important observed features. For example, an intense leading convective line and a broad stratiform rain region were simulated in both cases. Several well-known features associated with mid latitude squall lines, such as a squall mesohigh, a wake low, and a rear inflow, were also simulated in the two cases. These simulated features were much weaker in the tropical squall system than in the mid latitude one. Another difference is that stratiform rain developed rapidly for the tropical case. The model results also indicate that both the EMEX and PRE-STORM systems propagate by discrete growth of new convective elements ahead of the old cells. New growth originates along the leading edge of the gust front, which is propelled by downdraft air from decaying convective cells. These features have been reported in several field experiments (*e.g.*, GATE, TAMEX, COPT-81 and PRE-STORM).

Table 4 shows the individual components of the Q_1 and Q_2 budgets: condensation, evaporation, deposition, sublimation, melting, freezing, vertical eddy (heat and moisture) flux convergence and radiative cooling associated with

these two squall cases. These numbers are normalized with respect to their corresponding surface precipitation for comparison purposes. In the convective region of both squall systems, significant heating occurred from the latent heat released by condensation. In contrast, the condensation/deposition was nearly balanced by evaporation/sublimation in the stratiform and in the non-raining regions for the PRE-STORM case. A net heating in the stratiform region in the EMEX case is also a reflection of the greater stratiform rainfall generated in the EMEX case. The total amount of melted ice and frozen hydrometeors is comparable to the amount of evaporated rain. The contribution of freezing/melting processes to the Q_1 budget is small, because the latent heat of fusion is nearly an order of magnitude smaller than the latent heat of evaporation. This result is consistent with earlier work on GATE squall line simulation which applied continuous large-scale forcing (Tao and Simpson, 1989).

	(PRE-STORM Squall Line)				(EMEX9 Squall Line)				
	Total	Convective	Stratiform	Non-Raining		Total	Convective	Stratiform	Non-Raining
$\langle\bar{\rho}C\rangle$	1.47	1.13	0.27	0.07	$\langle\bar{\rho}C\rangle$	1.77	0.91	0.81	0.05
$\langle\bar{\rho}E\rangle$	0.69	0.24	0.36	0.09	$\langle\bar{\rho}E\rangle$	0.96	0.18	0.73	0.05
$\langle\bar{\rho}D\rangle$	0.74	0.22	0.33	0.19	$\langle\bar{\rho}D\rangle$	0.29	0.03	0.26	0.00
$\langle\bar{\rho}S\rangle$	0.47	0.07	0.18	0.22	$\langle\bar{\rho}S\rangle$	0.02	0.00	0.01	0.00
$\langle\bar{\rho}(C-E+D-S)\rangle$	1.05	1.04	0.06	-.05	$\langle\bar{\rho}(C-E+D-S)\rangle$	1.08	0.76	0.33	0.00
$\langle\bar{\rho}m\rangle$	0.12	0.05	0.07	0.00	$\langle\bar{\rho}m\rangle$	0.07	0.01	0.06	0.00
$\langle\bar{\rho}f\rangle$	0.09	0.06	0.03	0.00	$\langle\bar{\rho}f\rangle$	0.04	0.01	0.03	0.00
$\langle\frac{\partial\bar{\rho}w'\theta'}{\partial z}\rangle^1$	0.29	0.24	0.18	0.07	$\langle\frac{\partial\bar{\rho}w'\theta'}{\partial z}\rangle^1$	0.16	0.08	0.11	0.01
$\langle\frac{L_v}{C_p}\frac{\partial\bar{\rho}w'q_v'}{\partial z}\rangle^1$	0.95	0.92	0.78	0.17	$\langle\frac{L_v}{C_p}\frac{\partial\bar{\rho}w'q_v'}{\partial z}\rangle^1$	0.64	0.62	0.24	0.02
$\langle\bar{\rho}Q_R\rangle$	-.23	-.00	-.00	-.05	$\langle\bar{\rho}Q_R\rangle$	-.28	-.01	-.05	-.02

$\langle x\rangle = \int_x \int_{sfc}^{Z_{Top}} \int_{16h} (x)\Delta t \Delta z \Delta x$

[1]These vertical eddy heat and moisture convergence are absolute values.

Table 4 The individual components of the heating budget for (a) the PRE-STORM and (b) the EMEX squall lines, averaged over a 16 h simulation time and normalized with respect to their surface rainfall. See text for more information.

The eddy vertical heat and moisture convergence can only change the shape of the vertical profiles since the vertically integrated values are zero. Thus, absolute values are calculated in Table 4. The vertical eddy moisture flux is a major contributor to the model-derived Q_2 budget for both cases. This result is consistent with CRM studies with continuous large-scale forcing for both GATE squall and non-squall line simulations (Soong and Tao, 1980; Tao and Soong, 1986; Tao and Simpson, 1989 and many others), as well as with results from the CRMs without continuous large-scale forcing for a TAMEX squall line (Tao *et al.*, 1991) and from COPT-81 studies (Lafore *et al.*, 1988; Chong and Hauser, 1990). In contrast, the contribution of vertical eddy heat convergence was only about 10 per

cent of that due to latent heat release by condensation for the EMEX case and nearly 20 per cent for the PRE-STORM case. This difference is a result of the stronger vertical velocities associated with the PRE-STORM case. Another difference between these two cases is that the warm-rain processes were dominant in the tropical-oceanic squall case. Also note that the vertical eddy moisture flux is a major contributor to the model-derived Q_2 budget in the stratiform region for the PRE-STORM case as contrasted with the EMEX case. This behavior is a result of the drier PRE-STORM environment.

The vertical distribution of heating in the stratiform region of MCSs is considerably different from the vertical profile of heating in the convective region (Houze, 1982; Johnson, 1984). The modeled squall system is first partitioned into convective and stratiform regions following techniques developed by Churchill and Houze (1984). The Churchill and Houze separation technique is based on surface precipitation; therefore, two additional criteria have been added in order to further identify those grid points having no surface precipitation and which are not in the clear region. A grid point with no surface precipitation is considered convective if cloud water is present ($q_c > 0.1$ g kg^{-1}) below the melting layer, or if the maximum updraft exceeds 5 m s^{-1}. Both criteria are useful in identifying those regions where convection may be quite active aloft with little or no precipitation at the surface, such as areas associated with tilted updrafts and new cells initiated ahead of organized squall lines (Tao and Simpson, 1989). The Q_1 and Q_2 budgets derived in (3) and (4) are separated into three distinct cloudy regions: convective, stratiform and "non-raining" (the area where rainfall failed to reach the surface beneath the trailing stratiform cloud). Except for the radiative cooling term, the magnitude of each of the terms in the Q_1 and Q_2 budgets in clear air were small in comparison to those in the cloudy regions (Tao *et al.*, 1993).

Figure 4 shows Q_1 and Q_2 profiles for the convective and stratiform regions for the EMEX and PRE-STORM squall cases. The GCE simulated Q_1 and Q_2 profiles at the mature stage of the PRE-STORM case are in good agreement with those determined diagnostically using rawinsonde data (Gallus and Johnson, 1991; see Fig. 2). Overall, the Q_1 and Q_2 profiles for the simulated EMEX case are characteristic of tropical regions, and similar to the diagnostic study of AMEX cloud clusters by Frank and McBride (1989). Examination of Fig. 4 suggests that there are many common features in the Q_1 profiles between the squall lines, even though these systems occurred in very different geographic locations. For example, the convective heating is at a maximum in the lower and middle troposphere, and is largely due to net condensation in the convective updrafts. In contrast, the stratiform (anvil) heating is maximized in the upper troposphere, where it is dominated by ice deposition and cloud water condensation. Cooling is also taking place in the stratiform region beneath the melting layer predominately as a result of rain evaporation, although melting within a kilometer below the 0 ^{o}C level is also important. These features are well-known for mesoscale convective systems occurring in GATE, WMONEX, TAMEX, COPT-81 and PRE-STORM. The convective drying and stratiform moistening tend to offset each

other in the low levels in the Q_2 profiles for the PRE-STORM case. The mid-level minimum in the Q_2 profile for the EMEX case was due to vertical eddy transport in the convective region. The contribution to the total Q_1 budget by cloud-scale fluxes is minor for the EMEX case. In the PRE-STORM case, the total vertical eddy heat flux is quite important in the boundary layer and again in the middle troposphere. An even more significant contribution by vertical eddy transport to the Q_1 budget was found for a mid latitude supercell case (Schlesinger, 1990).

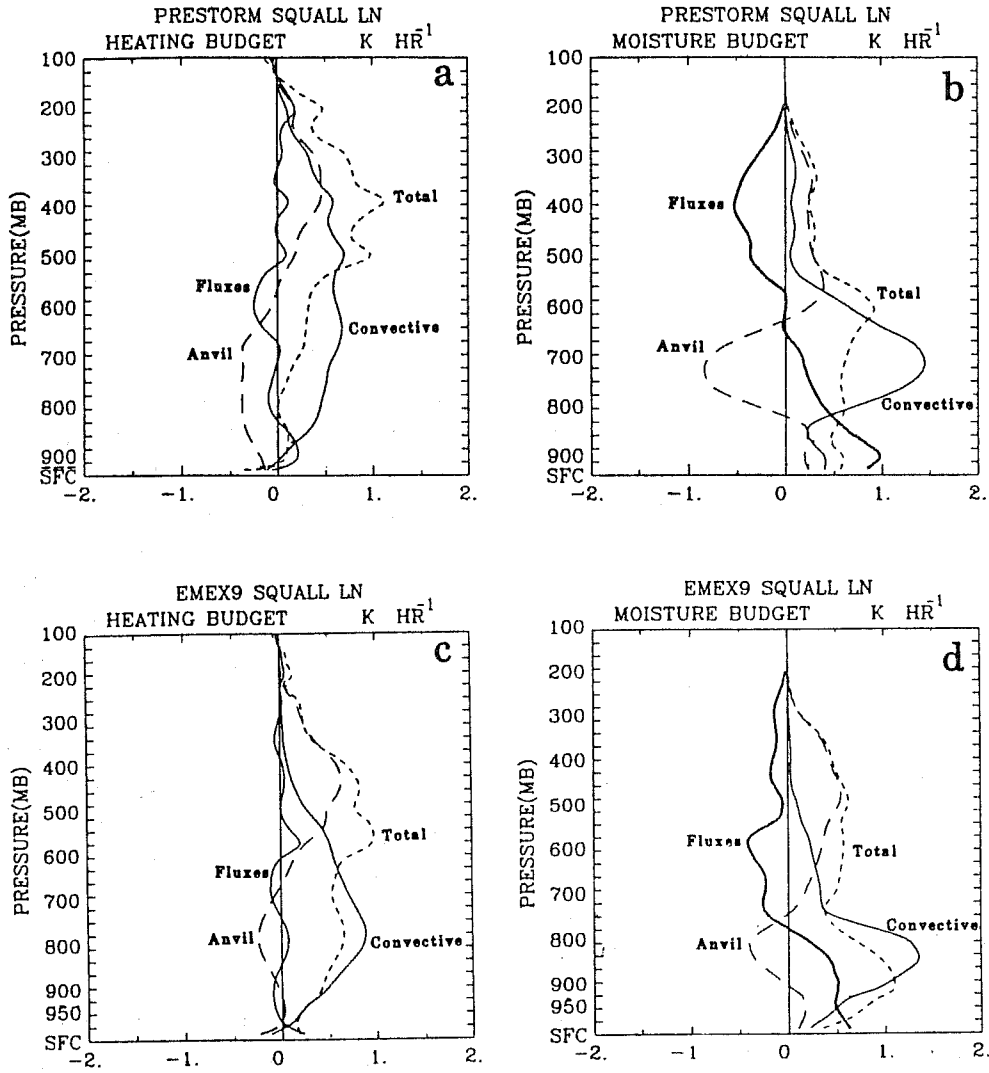

Fig. 4 ***(a)*** *The heating and* ***(b)*** *the moisture budgets for the PRE-STORM squall line averaged over a 16 h simulation time. The contributions by the convective region, the anvil region (stratiform and non-raining areas), and the total vertical eddy flux convergence (calculated over the convective and anvil regions) are also shown. The profiles for the convective and anvil regions also include the individual contributions due to vertical eddy flux convergence. Figs.* ***4(c)-(d)*** *are the same as* ***(a)-(b)****, except for the EMEX case. The vertical eddy flux convergence term includes both cloud scale and sub-grid scale (turbulence) effects.*

4. CRMs for Studying Cloud-Radiation Interactions and Climate Changes

The interaction between clouds and radiation is two-way. On one hand, clouds can reflect incoming solar and outgoing longwave radiation. Earth Radiation Budget Experiment (ERBE) results show that clouds can reflect a significant amount of shortwave radiation through the presence of large anvils (Ramanathan *et al.*, 1989) and non-precipitating low-level stratocumulus. It is thereby postulated that clouds presently have an overall net cooling effect on the earth. On the other hand, radiation can enhance or reduce cloud activity, particularly precipitation, and thereby the latent heat that is made available to the atmosphere. Recently, global change research has clearly indicated that it is necessary to understand the interactive processes associated with the radiative effects of clouds in order to properly address climate warming issues. CRMs have responded by incorporating both long- and short-wave radiative transfer processes which can then be used to study cloud-radiation interaction. It is often necessary to run the cumulus ensemble models for a long time and over a large domain so as to include the entire life cycle of many clouds and thus obtain results relevant to climate. Long time and large space requirements still limit most of these experiments to two dimensions, with a few three-dimensional tests.

Table 5 summarizes most of the previous cloud modeling studies associated with cloud-radiation interaction. They can generally be separated into three types based on their model setups and applications. For example, Held *et al.* (1993); Lau *et al.* (1993, 1994); Sui *et al.* (1994, 1995a), Xu and Randall (1995b) and Fu *et al.* (1995) applied cloud resolving models with cyclic lateral boundaries to study cloud-radiation interaction under different large-scale conditions (e.g., warm or normal sea surface temperature). Typically, an ensemble of cumulus clouds was generated by an imposed large-scale lifting and/or sensible and latent heat fluxes from the ocean. These studies were usually integrated for several days until modeled thermodynamic fields reached a quasi-equilibrium state. The second type of study quantifies the impact of cloud-radiation interaction upon a mesoscale convective system (i.e., Chen and Cotton, 1988; Tripoli and Cotton, 1989; Tao *et al.*, 1991; 1993; Chin, 1994; Chin *et al.*, 1995). Open lateral boundary conditions are applied and model integration is on the order of hours (about the life cycle of a squall line). The third type of study involves the use of regional scale models with 10-20 km horizontal resolution (i.e., Dudhia, 1989; Churchill and Houze, 1991; and Miller and Frank, 1993). Note that all of these modeling studies used two-dimensional models with large domains in order to resolve the stratiform region (or anvil). In addition, they all included ice processes for a more realistic simulation of the stratiform region. Strong two-way interaction between radiation and clouds is invariably found.

4.1 Cloud Radiation Interaction Mechanisms

It is known that longwave radiative processes can enhance precipitation in cloud systems. Three of the ways that longwave radiation is thought to interact with clouds are: 1) cloud-top cooling and cloud-base warming may alter the

	Model	Radiation	Cloud Optics	Domain & Horizontal Resolution	Lateral Boundary/ LargeScale Forcing	Model Inte-gration Time	Case
Chen & Cotton (1988)	2-D 3-Ice	Emissivity IR	Water	300 km (1.5 km)	Open/No Forcing	4 h	Mid. U. S. MCS
Dudhia (1989)	2-D 2-Ice Hydrostatic	Emissivity IR & SR	Water-Ice Size	700 km (10 km)	Constant Surface Pressure/N o Forcing	18 h	WMON EX
Tripoli & Cotton (1989)	2-D 2-Ice	Emissivity IR & SR	Water	~1200 km (1.08 km)	Open/No Forcing	16 h	Mid. U. S. MCS
Tao, Simpson & Soong (1991)	2-D 3-Ice	B. Band IR	Water-Ice Size	666 km (750 m-11km)	Open/Low-level Forcing	8 h	TAMEX Squall
Churchill & Houze (1991)	2-D 3-Ice	Emissivity IR & SR	Ice	260 km (10 km)	Fixed/ Forcing	Steady State	GATE
Tao, Simpson, Sui, Ferrier, Lang, Scala, Chou & Pickering (1993)	2-D 3-Ice	B. Band IR	Water-Ice Size	1025 km Stretched (750-1000m)	Open/No Forcing	16 h	EMEX PRE-STORM
Wong, Stephens & Stackhouse (1993)	2-D 3-Ice No-interaction	B. Band IR & SR	Water-Ice Size	500 km (1 km)	Open/No Forcing	6h	EMEX
Held, Hemler & Ramaswamy (1993)	2-D 3-Ice	B. Band IR & SR	Water	640 km (5 km)	Periodic/ No Forcing	42 days	Tropics
Sui, Lau, Tao, Simpson & Chou (1994)	2-D 3-Ice	B. Band IR & SR	Water-Ice Size	768 km (1500 m)	Periodic/ Forcing	52 days	West Pacific
Miller & Frank (1993)	2-D 2-Ice Hydrostatic	Emissivity IR & SR	Water-Ice Size	1240 km (20 km)	Periodic/ Forcing	24 h	Tropical (GATE)
Lau, Sui, Chou and Tao (1994)	2-D 3-Ice	B. Band IR & SR	Water-Ice Size Temperature	768 km (1500 m)	Periodic/ Forcing& No-Forcing	52 days	West Pacific
Chin (1994)	2-D 3-Ice	B. Band IR & SR	Water-Ice Size	3620 km (2 km - 40 km)	Open/No Forcing	8 h	Mid. U.S. Squall
Xu and Randall (1995)	2-D 3-Ice	B. Band IR & SR	Water-Ice Size	512 km (2 km)	Periodic/ Forcing	15 days	GATE
Fu, Krueger and Liou (1995)	2-D 3-Ice	B. Band IR & SR	Water-Ice Size Temperature	512 km (1 km)	Periodic/ Forcing	12 h	GATE
Chin, Fu, Bradley and Molenkamp (1995)	2-D 3-Ice	B. Band IR & SR	Water-Ice Size Temperature	3260 km (2 km-40 km)	Open/ Forcing	10 h	GATE
Dharssi, Kershaw and Tao (1996)	2-D 3-Ice	B. Band IR & SR	Water-Ice Size	756 km (750 m)	Periodic/ Forcing	16 h	EMEX

Table 5 Summary of previous cloud-radiation modeling studies. The general setup for each study is given along with some of the model characteristics and treatments used to parameterize the radiative effects. The case used in each study is also given.

thermal stratification of cloud layers, 2) differential cooling between clear and cloudy regions might enhance convergence into the cloud system, and 3) large-

scale cooling could change the environment. A two-dimensional version of the GCE Model has been used to perform a series of sensitivity tests to identify which is the dominant cloud-radiative forcing mechanism with respect to the organization, structure and precipitation processes for both a tropical (EMEX) and a mid-latitude (PRE-STORM) mesoscale convective system (Tao *et al.*, 1996).

The model results indicate that the dominant process for enhancing the surface precipitation in both the PRE-STORM and EMEX squall cases is the large-scale radiative cooling. However, the overall effect is really to increase the relative humidity and not the CAPE. Because of the high moisture in the tropics, the increase in relative humidity by radiative cooling can have more of an impact on precipitation in the tropical case than in the midlatitude case. The large-scale cooling led to a 36% increase in rainfall for the tropical case. The midlatitude model squall with a higher CAPE and lower humidity environment was only slightly affected (8%) by any of the longwave mechanisms. GCE model results also indicated that the squall systems' overall (convective and stratiform) precipitation is increased by turning off the cloud-top cooling and cloud-base warming. Therefore, the cloud-top cooling - cloud-base warming mechanism was not the responsible cloud-radiative mechanism for enhancing the surface precipitation. However, the circulation as well as the microphysical processes were indeed (slightly) enhanced in the stratiform region by the cloud-top cooling and cloud-base warming mechanism for the midlatitude squall case.

For both cases, the model results show that the mechanism associated with differential cooling between the clear and cloudy regions may or may not enhance precipitation processes. However, this mechansim is definitely less important than the large-scale longwave radiative cooling. Solar heating was run from 9 AM to 1 PM LST in both environments and was found to decrease the precipitation by 7% in each case, compared to the runs with longwave radiation only. This result suggests that solar heating may play a significant role in the daytime minimum/nighttime maximum precipitation cycle found over most oceans.

Table 6 lists the previous CRM studies that have investigated the impact of cloud-radiation interactive processes associated with various cloud systems. The increments in surface precipitation in Table 6 are normalized against the run without radiative processes. The conclusions associated with cloud-radiation mechanisms for our GCE modeled tropical (EMEX) and mid-latitude (PRE-STORM) squall cases are in good agreement with many previous modeling studies (listed in Table 6). For example, Xu and Randall (1995b), Miller and Frank, 1993 and Fu *et al.* (1995) on cloud-radiation mechanisms indicated that the differential cooling between cloudy and clear regions plays only a secondary role for enhancing the precipitation processes. Xu and Randall (1995b) and Fu *et al.* (1995) suggested that the cloud-top cooling and cloud-base warming destabilization mechanism could be important for prolonging the lifespan of high anvil clouds (around 10 km). Xu and Randall (1995b) showed that this direct cloud destibilization does not have any impact on surface precipitation. The previous modeling studies (Fu *et al.*, 1995 and Miller and Frank, 1993) also indicated that more surface precipitation can be generated in runs with constant clear-air radiative cooling than without. In addition, previous modeling results (Chin, 1994; Chin *et al.*, 1995; Miller and

Frank, 1993) indicated that solar radiative processes can reduce precipitation processes. However, the amount of increase or decrease in surface precipitation varies quite significantly among these different modeling studies, but only in regard to the tropical convective systems and not the mid-latitude systems. One possible explanation is that large-scale forcing (lifting) was needed in some of these different tropical convective system studies, and that imposed lifting varied from 2 cm/s to 14 cm/s in magnitude and was applied continuously or discontinuously in time among the different studies (see Table 7). Using an earlier version of the GCE model (Tao and Simpson, 1989b), which included a superimposed large-scale vertical velocity as the main forcing, sensitivity tests using two different large-scale vertical velocities were performed. These large-scale vertical velocities were applied throughout most of the troposphere (as Lau *et al.*, 1993; Sui *et al.*, 1994; Fu *et al.*, 1995; Xu and Randall, 1995). The results how that the radiative effects on the clouds, somehow, is quite sensitive to the imposed background ascent (or lifting). The larger the imposed vertical velocity (9-12 cm/s) there is, the lesser the impact of longwave cooling on surface precipitation processes (over 24 h of simulation time). This result can be easily explained using equation (10) such that when a larger large-scale advective forcing (lifting) is applied, a smaller sensitivity to radiative cooling is found. Frank and Miller (1993) also obtained a similar conclusion using a regional scale model. Also note that the larger the imposed vertical velocity, the larger the cloud coverage that was generated.

	LW Radiative Processes	Constant LW	LW & SW Radiative Processes	Imposed Lifting
Chen & Cotton	0%	No	No	No
Chin	11%	No	-7%	No
Tripoli & Cotton	N. A.	No	N.A.	No
Tao *et al.* 1995	8%	8%	-6%	No
Chin *et al.*	15%	No	-18%	2 cm/s Continuous
Fu *et al.* 1995	5%	15%	-1%	8-14 cm/s - Not Continous
Xu & Randall, 1995	N. A.	N. A.	N. A.	8-14 cm/s - Continuous
Tao *et al.* 1991	20%	No	No	4 cm/s - Not Continous
Tao *et al.* 1996	36%	2%	-7%	7 cm/s - Not Continous
Dharssi *et al*, 1996	30%	No	No	7 cm/s - Not Continous
Dudhia	36%	No	No	No
Churchill & Houze	0%	No	0%	Strong/Continuous
Miller & Frank	No	34%	18-21%	Strong/Continuous

Table 6 Summary of previous cloud-radiation modeling study results. The percentage increase or decrease in surface precipitation due to longwave and shortwave effects are given along with the mesoscale lifting, if used, for each case.

4.2 CRM and Climate Study

The representation of clouds and precipitation in CRMs is, perhaps, arguably superior to GCMs and climate models. This is because cloud models solve the primitive equations with much greater spatial and temporal resolution using more sophisticated and physically realistic parameterizations of cloud microphysical processes. In fact, a major limitation of global modeling still resides in the representation of clouds and their interactions with the radiation balance both locally and on the global scale[2]. Changes in the moisture distribution at middle and upper levels of the troposphere, as well as the radiative responses of cloud hydrometeors to outgoing longwave and incoming shortwave radiation, are a major factor in determining whether the earth system will warm or cool as the cloud systems respond to changes in their environment (Ramanathan *et al.*, 1989; Lindzen, 1990a,b; Betts, 1990; Lau *et al.*, 1993; Fowler and Randall, 1995b,c; Del Genio *et al.*, 1996). It is for this reason that GEWEX (Global Energy and Water Cycle Experiment) has formed the GCSS (GEWEX Cloud System Study) expressly for the purpose of studying these types of problems using CRMs.

Recently, cloud resolving models (CRMs) have been used to study the tropical water and energy cycles and their role in the climate system (Held *et al.*, 1993; Lau *et al.*, 1993, 1995, Sui *et al.*, 1994 and Grabowski *et al.*, 1996). The cloud resolving model does not need a cumulus parameterization scheme and it can allow explicit cloud-radiation interaction (cloud optical thickness is directly determined by cloud amount, phase of water species as well as the cloud size distribution; see Tao *et al.*, 1996). It is typically run for several weeks until modeled temperature and water vapor fields reached to a "*statistical equilibrium state*". However, two CRMs produced two different statistical equilibrium states even both used the same initial thermodynamic and wind conditions. Sui *et al* used the Goddard Cumulus Ensemble (GCE) model and found that the simulated climate is cool and dry (after 60 days of simulation). On the other hand, Grabowski *et al* used Clark model (19977) and CSU RAMS (Ref) found that their modeled climate was warm and humid after 24 day integration.

The initial conditions of Sui *et al* and Grabowski *et al* are from Marshall Island. There are still many differences among these two studies (see Table 7). Several sensitive tests have been performed and we will only present the runs that the "*physical processes*" to determine the climates from different CRMs simulations (Table 8).

Figure 5 shows the time series of the domain-averaged Temperature and water vapor for the seven experiments listed in Table 8. Clearly, there are two runs (Runs 6 and 7) that generally produced cool and dry "*quasi-equilibrium state*" after 14 day integration. In these two runs, the initial temperature, water vapor profiles as well as ocean surface temperature, respectively, from Sui et al and Grabowski et al are used. The *quasi-equilibrium state* of model climate in other five runs (Runs 1 to 5) is warm and humid. The major difference among these two groups of runs is whether allow convective processes to mix the horizontal

---

[2] The highest science priority identified in the Global Change Research Program (GCRP) is the role of clouds in climate and hydrological systems, which have been identified as being the most problematic issues facing global change studies.

wind and interact with the ocean surface are responsible for simulating different climate regimes. The results also indicated that microphysics and its interaction

	Sui, Lau, Tao & Simpson	Grabowski, Moncrieff & Kiehl
Surface P T, qv	1008 mb 28.18 C, 19.26 g/kg	1000mb 26.4 C, 18.3 g/kg
Ocean T	28.18 C	27.84 C
Forcing	Large-Scale W	Large-scale W*(dT/dz) & W*(dqv/dz)
Lx, Lz	768 km, 21.5 km	900 km, 24 km
DX, DZ	1500 m, 300-1000 m	1000 m, 200-500 m
Model Set-up	Mean horizontal wind Varies with Time (by convective mixing)	Mean horizontal wind is Constant
Advection Scheme	2nd-Order in Vertical & 4th-Order in Horizontal	Positive Definite Advection
Cloud-Radiation	No Diurnal Cycle Water/Ice Optical Properties	Diurnal Cycle Water Optical Properties
Microphysics	2 Water and 3 Ice	2 Water and 2 Ice

Table 7 Summary of differences in their respective model setups of Sui et al. (1994) and Grabowski et al. (1996).

Run	Sounding	Model - Setup	Mean U	Coriolis	Ice Processes
1	Grabowski, Moncrieff, Kiehl (NCAR)	Sui, Lau, Tao, Simpson (GSFC)	Constant	No	3 Classes (GSFC)
2	NCAR	NCAR	Constant	No	3 Classes
3	NCAR	NCAR	Constant	No	2 Classes
4	GSFC	GSFC	Constant	No	3 Classes
5	GSFC	GSFC	Constant	Yes	3 Classes
6	GSFC	GSFC	Varying	No	3 Classes
7	NCAR	GSFC	Varying	Yes	3 Classes

Table 8 Setups for the seven experiments conducted for examining the physical processes in determining warm/humid or cool/dry climate.

with radiation cannot alter the model simulated equilibrium state from one regime (warm/humid) to another (cold/dry); but it can change the degree of the equilibrium state (i.e., warm to warmer). In addition, these results showed that how the model is set-up to handle the prescribed large-scale forcing (vertical velocity) on T and q_v cannot change the modeled climate.

5. CRM for Understanding and Improving the Cumulus Parameterization

5.1 Convective and Stratiform Interactions

(a) CRM studies

One of the major findings from GATE is the important contribution of rainfall from mesoscale convective systems (MCSs). For example, Houze (1977)

estimated that four MCSs accounted for 50% of the rainfall at one of the GATE ships during Phase III. Another major finding is the widespread stratiform rain accounted for about 32%-49% of the total rainfall from these GATE MCSs. The fraction of stratiform rainfall from *midlatitude* squall lines can also be significant (29%-43%). The vertical distribution of heating in the stratiform region of MCSs is considerably different from the vertical profile of heating in the convective region (see Fig. 2). In addition, many recent studies indicated that a separation of convective and stratiform clouds is necessary for a successful surface rain and latent heating profile retrieval from remote sensors.

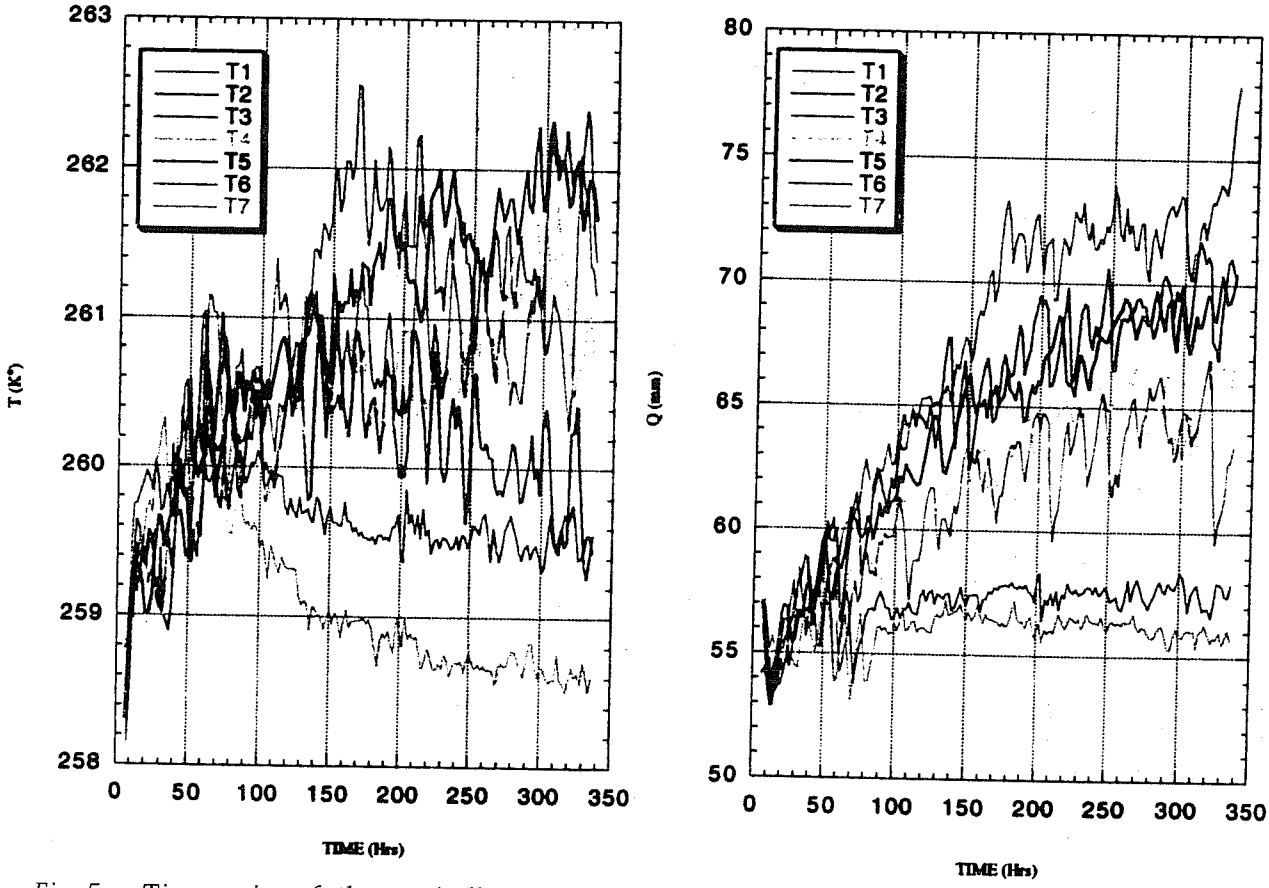

Fig. 5 *Time series of the vertically and horizontally averaged (a) mass-weighted temperature,* $<\overline{T}>$ *(K); (b) water vapor,* $<\overline{\rho q_v}>$ *(mm) for the 7 runs listed in Table 8.*

These findings lead to an important question: *what are the origins and growth mechanisms of particles in stratiform precipitation?* For example, Chen and Zipser (1982) suggested that both *depositional growth associated with upward motion in the anvil* and the *horizontal flux of hydrometeors from the convective region* are important in the maintenance of anvil precipitation. The CRM results can be used to quantitatively study the interaction between convective and stratiform regions by calculating their water budgets (see Table 9). For example, several organized convective systems (EMEX, TOGA COARE, TAMEX and

PRESTORM) which were occurred in different large-scale environments have been simulated using the GCE model (Tao *et al.*, 1993; Tao, 1995). The horizontal transfer of hydrometeors from the convective to the stratiform regions occurs mainly in the middle troposphere for the EMEX and TOGA COARE squall line MCSs. By contrast, two thirds of the horizontal transfer of hydrometeors is accomplished in the upper troposphere for the PRE-STORM case. Also a more vigorous transfer of hydrometeors in the lower troposphere from the stratiform region back into the convective region occurs for the PRE-STORM case. For the TAMEX case, the horizontal transfer of hydrometeors can occur at both middle and upper troposphere. A downward transfer of hydrometeors from the middle to the lower troposphere is a dominant process in the stratiform regions for all four cases (see Fig. 6).

	Model	Type	Radiation	Domain	Integration	Case
Rutledge (1986)	3-D	Kinematic	No	180x 130 km^2	Steady State	GATE
Rutledge & Houze (1987)	2-D	Kinematic	No	128 km	Steady State	Oklahoma Squall Line
Lafore & Moncrieff (1989)	2-D	Time-Dependent	No	480 km Nesting	12 h	COPT 81
Churchill & Houze (1991)	2-D	Kinematic	SR & IR	260 km	Steady State	GATE Squall Line
Tao, Simpson, Sui, Ferrier, Lang, Scala, Chou & Pickering (1993)	2-D	Time-Dependent	IR	1025 km Stretched	16 h	EMEX & PRE-STORM
Sui, Lau, Tao, Simpson & Chou (1994)	2-D	Time-Dependent	SR & IR	768 km	1248 h	West Pacific
Caniaux et al (1994)	2-D	Time-Dependent	No		8 h	COPT 81
Chin (1994)	2-D	Time-Dependent	SR & IR	768 km	12 h	Midlatitude
Chin et al. (1995)	2-D	Time-Dependent	SR & IR	768 km	12 h	GATE

Table 9 Summary of previous convective and stratiform interaction modeling studies. The general setup (i.e., kinematic or time dependent) for each study is given along with some of the model characteristics and treatments used to parameterize the radiative effects. The case used in each study is also given.

The contribution to stratiform rain by the convective region has to be quantified in order to help improve the cloud parameterization for large scale model. This can be done by estimating a ratio (**R**), $\mathbf{R}=C_T/(C_T+C_m)$, where C_T is the horizontal transfer of hydrometeors from the convective region into the stratiform region above the 10 ^oC level, and C_m is the sum of the net condensation in the stratiform region and in the non-raining region above the 10 ^oC level. *A small ratio indicates that the horizontal transfer of hydrometeors*

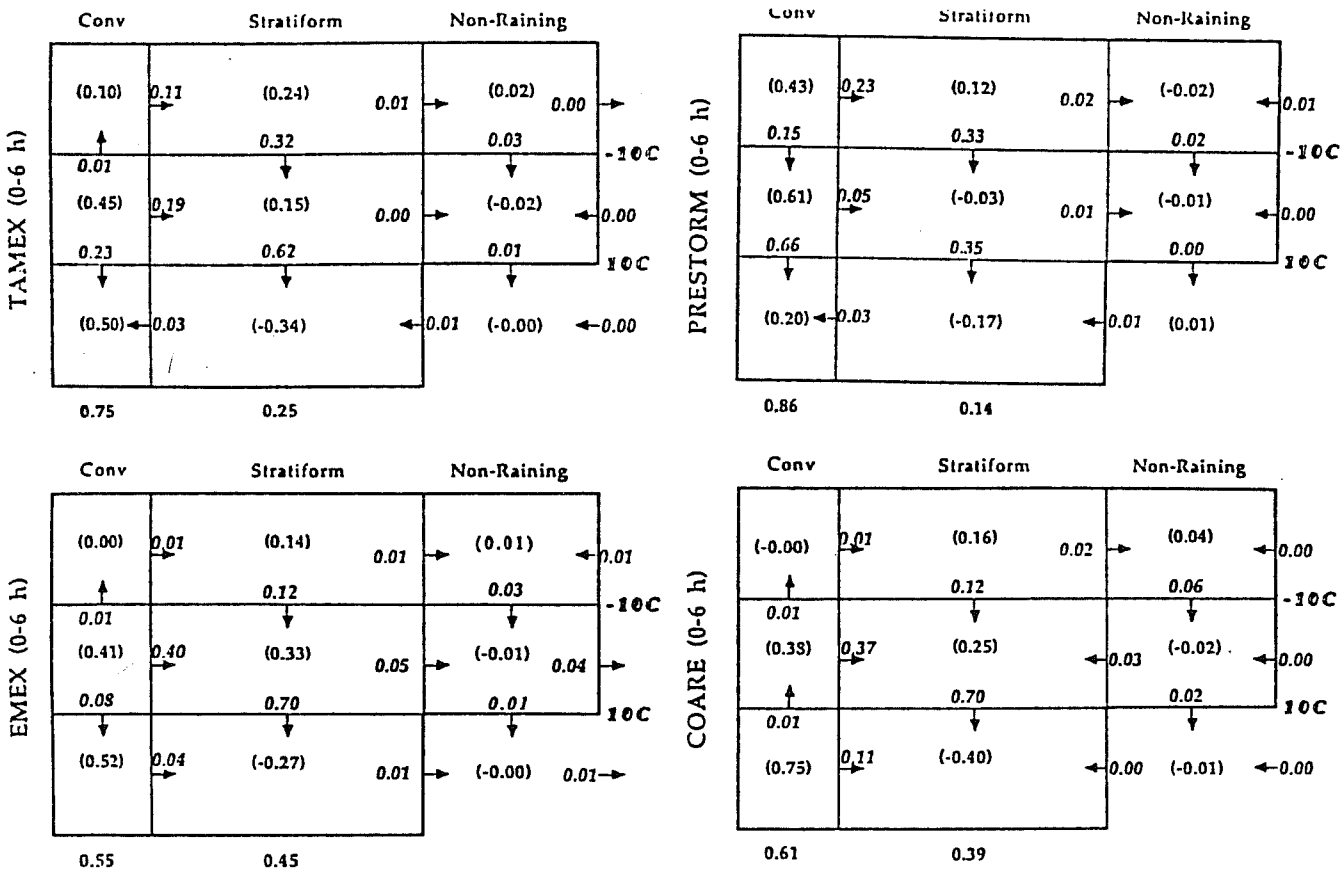

Fig. 6 The water budgets for (a) TAMEX, (b) EMEX, (c) PRE-STORM and (d) TOGA COARE simulated squall-line MCSs. Italic numbers indicate the amount of condensate transfer between various regions and layers while quantities in parenthese are the net condensation generated through microphysical processes.

from the convective region is a small source of condensate for the stratiform anvil, whereas a ratio near unity indicates that nearly all of the condensate in the stratiform region was transported from the convective region. All five cases showed large ratios (range from 0.33 to 0.82) and these results imply the role of convective region in the generation of stratiform rainfall can not be neglected (Table 10). The relative importance of the horizontal transfer processes to the stratiform water budget is similar between the initial and the mature stages of the West Pacific TAMEX, TOGA COARE and EMEX systems. In contrast, during the initial stage of the PRE-STORM simulation, nearly all of the condensate in the stratiform region was a result of the horizontal transport from the convective region. As the PRE-STORM system matured, the contribution made by the horizontal transport of hydrometeors from the convective region (*i.e.*, the ratio R) decreased, such that the sources of condensate in the stratiform water budget were similar for both of the mature storms. It is hypothesized that during the initial stage of the PRE-STORM simulation, much of the condensate transported from the convective region is used to moisten and modify the dry environment at

middle and upper levels. Condensation and deposition become increasingly more important with time in the stratiform water budget once the larger-scale environment reaches saturation. This evolution in the stratiform water budget is less obvious in the TAMEX, TOGA COARE and EMEX cases because the environment is much more moist.

	Stratiform (0-12 h)	Ratio (0-12 h)	Initial-Stage (0-6 h)	Mature-Stage (6-12 h)
COARE	42.3%	0.40	0.46	0.36
EMEX	49.1%	0.41	0.47	0.35
TAMEX	29.6%	0.37	0.43	0.33
PRESTORM	22.5%	0.54	0.82	0.43
W. Pacific*	41.3*%	0.62*	0.61*	0.66*

Table 10 Values of the ratio R for the CRM simulations of several convective systems, as well as for the 6 h periods corresponding to the initial and mature stages. Also their respective stratiform rain components is shown in the first column.

In Table 11, the ratios in Table 10 are compared against those determined from observational studies of composite wind and thermodynamic fields for five different GATE MCSs (Leary and Houze, 1980; Gamache and Houze, 1983), a midlatitude squall line (Gallus and Johnson, 1991), and a tropical-continental squall line (Chong and Hauser, 1989). For six out of the seven observed cases the ratio is very close to or above 0.50. This implies that the convective region plays a very important role in the generation of stratiform rain. Very good agreement is evident between the ratio at the mature stage of the modeled PRE-STORM squall system and that estimated by Gallus and Johnson (1991). The modeled EMEX, TOGA COARE cases indicate that a relatively small contribution (0.37) to stratiform formation can be attributed to the horizontal transfer of condensate from the convective region. Stratiform cloud formation occurs earlier due to the very moist environmental conditions at the middle and upper levels associated with the EMEX case (Fig. 6b). Nevertheless, a direct comparison between these studies and the current model study should be done with caution, because a different spatial resolution and a different definition for the convective-stratiform region was used here. The comparison between the simulated PRE-STORM and EMEX cases, however, is consistent because the same type of data set and the same criteria for partitioning the convective and stratiform regions are used.

Case	Anvil Portion	Ratio
LH-A	0.40	1.00
LH-B	0.40	1.00
LH-C	0.40	0.50
GH-1	0.49	0.55

GH-2	0.49	0.64
GJ-June 10	0.30	0.37
COPT81	0.40	0.47

Table 11 The same ratio defined in Table 10 except for different MCS cases, A, B and C of Leary and Houze (1980), cases I and II of Gamache and Houze (1983, the 10-11 June squall line of Gallus and Johnson (1991), and the COPT squall line of Chong and Hauser (1989). (From Tao et al., 1993)

In Table 12, the ratios in Table 10 are compared against those determined from other CRM results listed in Table 9 (Chin, 1994; Chin *et al.*, 1995; Caniaux *et al.*, 1995) and a GCE simulation with 52 day integration (Sui *et al.*, 1994). Very good agreement is evident between the ratio at the mature stage of our modeled EMEX and TOGA COARE squall systems and that estimated by Chin *et al.* (1995). Note that a tropical squall case was also studiedby Chin *et al.*. The comparison between our simulated PRE-STORM and other CRM simulated midlatitude cases (Chin, 1994; and Caniaux *et al* , 1994), however, is quite different. Their simulations may underestimate the contribution by the horizontal transfer of hydrometeors from the convective region (see the ratios shown in Table 11).

	Ratio	**Stratiform Amount (%)**	**Case**
Chin (1994)	115-119% (2 km) 65-68% (6 km)	10%	Midlatitude
Chin *et al* (1995)	33-40% (3.6 km)	33-44%	Tropics (GATE)
Sui *et al* (1994)*	80% (4 km)	32%	West Pacific
Caniaux *et al* (1994)	22% (4-5 h) 9% (7-8 h)	17% 44%	COPT 81

Table 12 The same ratio defined in Table 10 except for previous CRM studying of convective and stratiform interaction.

b. The Convective and Stratiform Processes in the Large-Scale Models

Molinari and Dudek (1992) and Frank (1993) suggested that the best approach to cumulus parameterization in regional scale models (30-120 km horizontal resolution, 150-300 seconds time step) appears to be "*to use a scheme that operates simultaneously with and interacts explicitly with the explicit scheme (grid scale microphysical processes)*". They termed such schemes "*hybrid schemes*". The hybrid approach (by separating out the forcing mechanism for the mesoscale component) is to resolve the "mesoscale" circulations and microphysical processes that direct influence the development of the "stratiform clouds". The cumulus parameterization makes use of steady-state cloud model that interacts with grid-scale variables and provides with the net heating, drying, and condensate associated with "convective cells". The interaction between parameterized and explicit resolved cloud processes is through the "detrainment"

of water vapor (or/and condensate") generated from a steady-state cloud model into the "resolved" stratiform clouds.

Recently, GCMs and climate models (i.e., CSU GCM and GISS GCM) allow both a cumulus parameterization scheme and an explicit moisture scheme to be activated simultaneously in the model simulations. The cumulus parameterization scheme is generally used to represent convective precipitation (10 km spatial scale) and the explicit moisture scheme to represent grid-resolvable precipitation such as stratiform/cirrus clouds (100-200 km spatial scale). CSU GCM has been implemented an explicit microphyiscal scheme with *five* prognostic variables for the mass of water vapor, cloud water, cloud ice, rain and snow. GISS global climate model has added an efficient prognostic cloud water (one species only). Both schemes allow for life cycle effects in stratiform clouds and permit cloud optical properties to be determined interactively. Stratiform clouds can be coupled with parameterized convection through detrainment of cloud water and/or cloud ice from the "tops" of cumulus towers or at any level above the 550 mb level.

The explicit interaction between cumulus parameterized and grid-scale resolved microphysics is only one-way. Noted that some water condensate generated by stratiform rain can be transported into convective region. In additon, how much (all or partial) and where (cloud tops or above melting layer) of parameterized water condensate should detrain into the explicit resolved microphysical scheme need to be addressed. In future, the CRM results can be used for improving the cumulus parameterization schemes (GCSS Science Team Report) as well as for understanding the interaction between the cumulus parameterization scheme and the explicit moisture scheme. For example, CRMs can study the time evolution of each of the water budget terms associated with MCSs in different geographical regions, as well as to determin whether any important variations in the evolution of the water budget can be explained in terms of differences in the wind and thermodynamic characteristics of the large-scale environments.

5.2 Precipitation Efficiency

Different definitions of storm precipitation efficiency were investigated from numerical simulations of convective systems in widely varying large-scale conditions (COHMEX and GATE) using a CRM with sophisticated, two-moment bulk ice microphysics (Ferrier *et al.*, 1996). The model results indicate that the vertical orientation of the updrafts, which is controlled by the vertical wind shear, and the ambient moisture content are important in determining storm efficiency. The radar reflectivity structure and organization of the convection is displayed in Fig. 7 for four of the model runs listed in Table 1. The convective cores in run C were vertically erect during the first 4 h, thereafter developed slight downshear tilt[3] that was most evident at middle and upper levels as an extensive anvil spread

[3] The orientation or tilt of the convection is defined relative to the low-level wind shear vector below 600 mb in run C, 875 mb in run G-SS, and 700 mb in runs G, C-GW, and G-90.

ahead of the convection. The systems were tilted upshear in runs G and C-GW in response to the easterly jet near 700 mb[4]. A series of runs were made varying the shear profiles, and the shallow wind shear in run G-SS supported the development of a narrow, nearly upright convective system that was long lived.

Run	Description
C	COHMEX simulation - Downshear Convection
G	GATE Simulation - Upshear Convection
C-GW	COHMEX thermodynamics with GATE winds - Upshear Convection
G-90	GATE run with 90% relative humidity above 875 mb - Upshear Convection
G-SS	GATE thermodynamics with strong, shallow shear - Erect Storm

Table 13 Summary of model experiments .

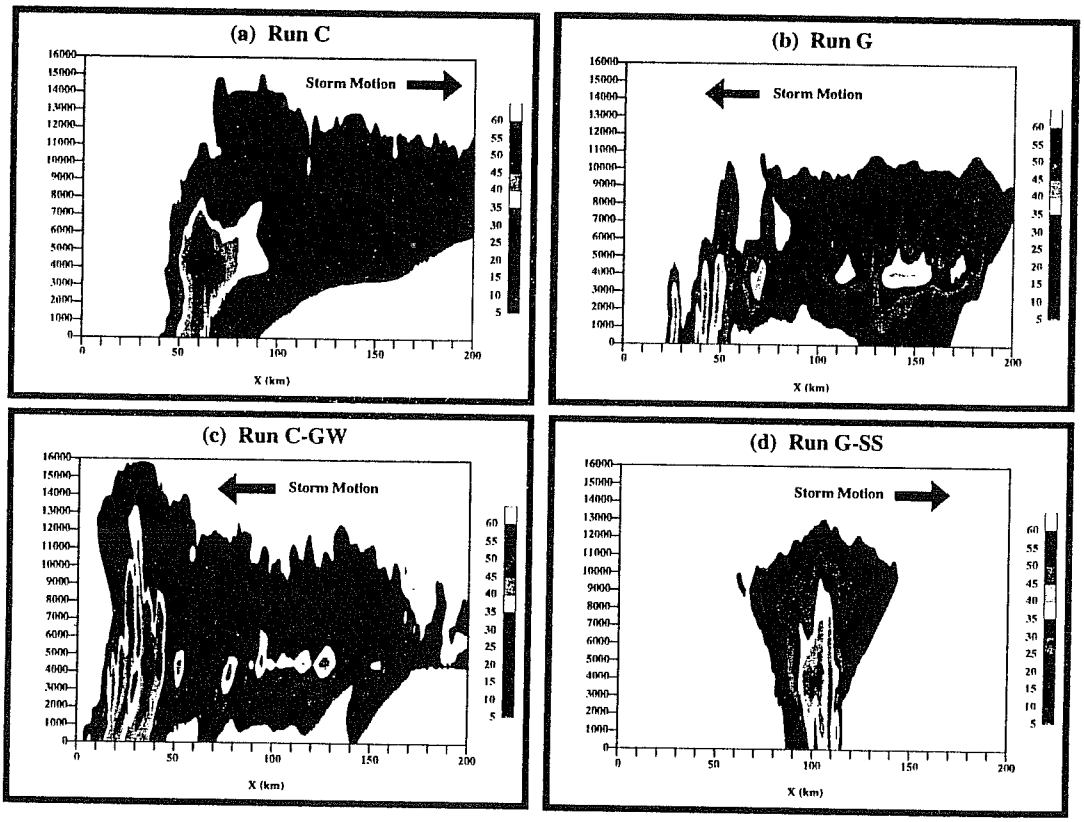

Fig. 7 Radar reflectivity fields over a 200-km wide portion of the domain for (a) run C, (b) run G, (c) run C-GW, and (d) run G-SS at the end of the 6-h model simulations. Direction of storm motion is indicated by the bold arrows.

In field observational studies, precipitation efficiency is usually defined as:

4 Radar echoes are most often vertical in orientation even when the clouds are observed to slant significantly in the horizontal (e.g., Warner *et al.*, 1980; Zipser *et al.*, 1981).

$$\mathbf{PE} = \frac{\mathbf{R}}{\mathbf{VI}} \tag{7}$$

where VI is the inflow of water vapor into the storm through cloud base. Braham (1952) estimated PE_V of approximately 10 percent for small airmass thunderstorms. However, the mass fluxes of inflow air into these storms were one to two orders of magnitude smaller than in subsequent studies which cited precipitation efficiencies ranging from 20 to 120 percent (e.g., Newton, 1963, 1966; Auer and Marwitz, 1968; Marwitz, 1972; Foote and Fankhauser, 1973; Gamache and Houze, 1983; Heymsfield and Schotz, 1985; Fankhauser, 1988; Chong and Hauser, 1989). Some of these investigations suggested that PE_V decreases with increasing ambient shear (e.g., Marwitz, 1972; Foote and Fankhauser, 1973), in which PE was estimated to vary from 100 to 20 percent for increasing shear magnitudes from $2x10^{-3}$ to $4.5x10^{-3}$ s^{-1}, respectively (Foote and Fankhauser, 1973). This inverse relationship between PE and shear has been incorporated as a closure assumption in some cumulus parameterization schemes (Fritsch and Chappell, 1980; hereafter FC).

However, more recent estimates of PE for CCOPE thunderstorms (Cooperative Convective Precipitation Experiment) by Fankhauser (1988) failed to show the inverse functionality between shear and PE. In fact, there was a small positive correlation between PE and the strength of the low-level shear and the low-level water vapor content, although no clear relationship of PE with any environmental factor was identified. Citing limitations in aircraft instruments and sampling, Fankhauser also noted that PE may have been overestimated in some of the earlier studies as a result of underestimates in the lateral inflow of water vapor into the storms.

Precipitation efficiencies determined from closure assumptions used in some of the cumulus parameterization schemes are listed in Table 14. The first two efficiency parameters, PE_{FC} and PE_{ZF}, were used in the closure assumptions of the FC cumulus parameterization and a modification of the FC scheme by Zhang and Fritsch (1986), respectively. In FC an empirical relationship between precipitation efficiency and ambient shear over the depth of the cloud column (Marwitz, 1972; Foote and Fankhauser, 1973) is used to determine the fraction of condensate produced in updrafts that is lost by evaporation in downdrafts. The quantity PE_{FC} in Table 14 is the precipitation efficiency obtained from this empirical relationship, but modified slightly for an assumed cloud-top height of 12 km. In an updated version of the FC scheme, Zhang and Fritsch (1986) estimated PE from averaging two different empirical relationships based on cloud-base height and the mean shear over lower levels. The estimates of PE_{AK} in Table 14 are based on the Kuo (1974) cumulus parameterization, in which values of PE are equal to (1-b) with b representing the fraction of condensate produced in convective updrafts lost by evaporation (often termed the moistening parameter). Using the empirical relationship for parameter b proposed by Anthes (1977), the mean humidity was obtained from the input soundings by integrating vertically the relative humidity with respect to water and ice at temperatures above and below 0°C, respectively, between cloud base and a height of 12 km. With the

exception of run C, values of PE_{AK} were typically much higher than the storm efficiencies determined from the model.

Run	Stratiform Rain (%)	PE Fritsch & Chappell	PE Zhang & Fritsch	PE Zhang & Fritsch*	PE Kuo/ Anthes
COHMEX **Downshear**	5	33	58	33	40
GATE **Upshear**	25	46	55	28	61
COHMEX- GATE Wind **Upshear**	29	46	54	25	40
GATE- 90% RH above 850 mb **Upshear**	27	46	55	28	82
GATE - Strong/shallow shear **Erect**	10	90	64	45	61

Table 14 Precipitation efficiencies (percent) determined for each of the 5 different runs based on closure assumptions used in different cumulus parameterization schemes (see text). The fraction of total rain from stratiform precipitation is also shown.

Different definitions of storm precipitation efficiency are also investigated. The total precipitation efficiency (PE_t) in the simulations can be defined as the ratio of the total rainfall to the total condensation,

$$\mathbf{PE_t = \frac{R_t}{C_t}} \tag{8}$$

where C_t is the total condensation (condensation onto water plus deposition onto ice for all hydrometeor species). A similar definition of precipitation efficiency was adopted in the three-dimensional modeling study of Weisman and Klemp (1982), in which precipitation efficiencies varied from 11 to 49 percent over the 2-h duration of their simulations. Finally, a rain efficiency (PE_r) parameter is derived that estimates the total production of rain that results in surface rainfall and which is not lost due to evaporation. It is obtained by from the total continuity equation for rain (eq. A.4 in Ferrier, 1994),

$$\mathbf{PE_r = 1 - \frac{E_r}{(A_{rw} + SH_x - A_{xr})}} \tag{9}$$

The term A_{rw} represents the total conversion from cloud water to rain by autoconversion and collection processes, SH_x is the total mass of liquid water shed from wet precipitation ice, A_{xr} is the freezing of rain due to collisions with ice, and E_r is the total rain evaporation.

Table 15 shows the inflow of water vapor (VI) into the leading edge of the storms obtained for different assumed inflow depths. Two different sets of inflow depths (Z_{in}) were used in the calculations. The first set of inflow depths was based on the simulated cloud base heights, which was below a height of 1 km in all cases. The second set of inflow depths was based on the model level closest to a height of 2 km, which is the supply of moisture into the updrafts as assumed in FC. Tracer

analyses of this GATE case (Nicholls and Weissbluth, 1988) and other convective systems (Lafore and Moncrieff, 1989; Scala *et al.*, 1990; Pickering *et al.*, 1992) have also shown that non-negligible amounts of air above cloud base are incorporated into the updrafts. As expected estimates of PE can differ substantially for various assumed inflow depths. The precipitation efficiencies, PEt and PEr, are also shown in Table 15.

Run	PE dp=0.5 km	PE dp=1.9 km	PE dp=11.8 km	PE_r	PE_t
COHMEX **(Downshear)**	66	33	26	76	45
GATE **(Upshear)**	106	33	22	57	25
COHMEX- GATE Wind **(Upshear)**	83	30	17	55	24
GATE- 90% RH above 850 mb **(Upshear)**	59	52	37	64	34
GATE - Strong/shallow shear **(Errect)**	97	59	49	67	39

Table 15 Precipitation efficiencies (PE in percent) calculated for two sets of assumed inflow depths (near cloud base and near 2 km) and for most of the troposphere below 12 km (dp in km). PEs (PEr and PEt) from two different definitations of storm efficiency were also shown.

The vertical orientation of the updrafts and the ambient moisture content are the major factors that determine the precipitation efficiency of a storm. In terms of defining precipitation efficiency as the rainfall divided by condensation, vertically erect updrafts promote the most effective collection of cloud condensate by rapidly falling precipitation species. Because upshear sloping convection possesses deeper and broader areas of subsaturation, the evaporative loss of rain is greater than in downshear-tilted and erect storms. These conclusions are valid even when different methods were used to calculate total storm condensation. The reduced efficiency of upshear convection is manifested primarily by increased cloud water evaporation along the upshear edge of the updrafts at middle levels, as well as by enhanced fluxes of water vapor and condensate rearward from the convective region. These processes aid the development of trailing stratiform precipitation. Yet, stratiform precipitation is quite inefficient due to evaporation of rain in the subsaturated mesoscale downdraft at low levels and the sublimation of snow and ice crystals in the trailing portion of the stratiform anvil. In fact, net deposition above the freezing level was confined to the first 50 to 70 km of the simulated storms. Thus, the increasing contribution of stratiform precipitation to total rainfall as the systems slanted more in the upshear direction is consistent with their being less efficient.

Although downshear tilted convection is quite efficient in terms of the rainfall divided by condensation, it is less efficient when defined in terms of the

flux of water vapor into the storm. The simulations suggest that the gust fronts are too weak to block all of the low-level inflow, causing some of the ambient air to pass through the cold pool without being carried up into deep updrafts. Vertically erect storms, however, are the most efficient based on all criteria for defining precipitation efficiency. Relatively minor modifications in the upper-level winds produced very large variations in the intensity and efficiency of the COHMEX simulations due to a transition from downshear to upshear convection. Precipitation efficiency is higher in moist versus drier environments as a result of larger condensation rates, whereas variations in cloud and rain evaporation rates are much smaller. Since the ambient moisture affects storm condensation through the vertical advection of water vapor, the development and intensity of convection is strongly modulated by the height and depth of dry layers above the boundary layer. Furthermore, the degree of modulation is expected to increase for environments with weaker thermodynamic instability.

None of the closure assumptions tested showed consistent agreement with any of the precipitation efficiency parameters diagnosed from the simulations. The results of this study suggest that: (1) the effects of ambient wind shear and moisture content throughout the depth of the troposphere need to be considered in the calculations of PE in cumulus parameterization schemes; (2) the primary role of wind shear (and, to a lesser extent, environmental instability) that affects PE appears to be through determining the vertical orientation of the updraft regions. The relative contribution of stratiform precipitation to total storm rainfall also needs to be considered in models with coarse horizontal grid resolution.

6. Acknowledgement

The authors thank Mr. S. Lang for reading the manuscript and for providing many comments. The work is supported by the NASA Headquarters Physical Climate Program, the NASA Tropical Rainfall Measuring Mission (TRMM) and the Interdisciplinary Investigation of the Earth Observing System (EOS). These authors are grateful to Drs. R. Kakar and K. M. Lau for their support of this research. Acknowledgment is also made to NASA/Goddard Space Flight Center for computer time used in the research.

8. References

Abramopoulos, F., C. Rosenzweig, and B. Choudhury, 1988: Improvedground hydrology calculations for global climate models (GCMs): Soil water movement andevapotranspiration. *J. Climate*, **1**, 921-941.

Ackerman, T. P., K.-N. Liou, F. P. J. Valero and L. Pfister, 1988:Heating rates in tropical anvils. *J. Atmos. Sci.*, **45**, 1606-1623.

Adler, R. F., H.-Y. Yeh, N. Prasad, W.-K. Tao and J. Simpson,1991: Microwave rainfall simulations of a tropical convective system with a three-dimensional cloudmodel. *J. Appl. Meteor.*, **30**, 924-953.

Adler, R. F., A. J. Negri, P. R. Keehn, and I. M. Hakkarinen,1993: Estimation of Monthly Rainfall over Japan and Surrounding Waters from a Combination ofLow-Orbit Microwave and Geosynchronous IR Data. *J. Appl. Meteor.*, **32**, 335-356.

Anthes, R. A., 1977: A cumulus parameterization scheme utilizinga one-dimensional cloud model. *Mon. Wea. Rev.*, **105**, 270-286.

Auer, A. H., Jr., and J. D. Marwitz, 1968: Estimates of air andmoisture flux into hailstorms on the High Plains. *J. Appl. Meteor.*, **7**, 196-198.

Avissar, R., and R. A. Pielke, 1989: A parameterization ofheterogeneous land-surface for atmospheric numerical models and its impact on regionalmeteorology. *Mon. Wea. Rev.*, **117**, 2113-2136.

Betts, A. K., 1990: Greenhouse warming and the tropical watervapor budget. *Bull. Amer. Meteor. Soc.*, **71**, 1465-1467.

Braham, R. R., Jr., 1952: The water and energy budgets of thethunderstorm and their relation to thunderstorm development. *J. Meteor.*, **9**, 227-242.

Caniaux, G., J.-L. Redelsperger, and J.-P. Lafore, 1994: Anumerical study of the stratiform region of a fast-moving squall line. Part I: General description andwater and heat budgets. *J. Atmos. Sci.*, **51**, 2046-2074.

Cess, R. D., M. H. Zhang, P. Minnis, L. Corsetti, E. G. Dutton,B. W. Forgan, D. P. Garber, W. L. Gates, J. J. Hack, E. F. Harrison, X. Jing, J. T. Kiehl, C. N.Long, J.-J. Morcrette, G. L. Potter, V. Ramanathan, B. Subasilar, C. H. Whitlock, D. F. Young, and Y.Zhou, 1995: Absorption of solar radiation by clouds: Observations versus models. *Science*, **267**, 496-499.

Chen, Y.-L., and E. J. Zipser, 1982: The role of horizontaladvection of hydrometeors in the water budget of a large squall system. *Preprints, 12th Conf. on Severe Local Storms*, San Antonio, Amer. Meteor. Soc., 355-358.

Chen, S., and W. R. Cotton, 1988: The sensitivity of a simulatedextra-tropical mesoscale convective system to longwave radiation and ice-phase microphysics. *J. Atmos. Sci.*, **45**, 3897-3910.

Chin, H.-N. S., 1994: The impact of the ice phase and radiationon a mid-latitude squall line system. *J. Atmos. Sci.*, **51**, 3320-3343.

Chin, H.-N. S., Q. Fu, M. M. Bradley, and C. R. Molenkamp, 1995:Modeling of a tropical squall line in two dimensions and its sensitivity to environmental winds andradiation. *J. Atmos. Sci.*, **52**, 3172-3193.

Chong, M., and D. Hauser, 1989: A tropical squall line observedduring the COPT 81 experiment in west Africa. Part II: Water budget. *Mon. Wea. Rev.*, **117**, 728-744.

Chong, M. and D. Hauser, 1990: A tropical squall line observedduring the COPT 81 experiment in West Africa. Part III: Heat and moisture budgets. *Mon. Wea. Rev.*, **118**, 1696-1706.

Chou, M.-D., 1990: Parameterization for the absorption of solarradiation by O_2 and CO_2 with application to climate studies. *J. Climate*, **3**, 209-217.

Chou, M.-D., 1992: A solar radiation model for use in climatestudies. *J. Atmos. Sci.*, **49**, 762-772.

Chou, M.-D., and M. J. Suarez, 1994: An efficient thermalinfrared radiation parameterization for use in general circulation models. NASA Tech. Memo. 104606, **3** , 85 pp.

Chou, M.-D., A. Arking, J. Otterman, and W. L. Ridgway, 1995: Theeffect of clouds on atmospheric absorption of solar radiation. *Geophy. Res. Lett.*, **22**, 1885-1888.

Churchill, D. D., and R. A. Houze, Jr., 1984: Development andstructure of winter monsoon cloud clusters on 10 December 1978. *J. Atmos. Sci.*, **41**, 933-960.

Churchill, D. D., and R. A. Houze, Jr., 1991: Effects ofradiation and turbulence on the diabatic heating and water budget of the stratiform region of a tropicalcloud cluster. *J. Atmos. Sci.*, **48**, 903-922.

Clark, T. L., 1979: Numerical simulations with athree-dimensional cloud model: lateral boundary condition experiments and multicellular severe storm simulations. *J. Atmos. Sci.*, **36**, 2191-2215.

Cox, S. K., and K. T. Griffith, 1979: Estimates of radiativedivergence during Phase III of the GARP Atlantic Tropical Experiment: Part II. Analysis of Phase IIIresults. *J. Atmos. Sci.*, **36**, 586-601.

Crook, N. A., and M. Moncrieff, 1988: The effect of large-scaleconvergence on the generation and maintenance of deep moist convection. *J. Atmos. Sci.*, **45**, 3606-3624.

Del Genio, A. D., M.-S. Yao, W. Kovari and K. K.-W. Lo, 1996: Aprognostic cloud water parameterization for global climate models. *J. Climate*, **9**, 270-304.

Dharssi, I., R. Kershaw, and W.-K. Tao, 1996: Longwave radiativeforcing of a simulated tropical squall line. *Quart. J. Roy. Meteor. Soc.*, **123**, 187-206, 1997.

Dudhia, J., 1989: Numerical study of convection observed duringthe Winter Monsoon Experiment using a mesoscale two-dimensional model. *J. Atmos. Sci.*, **46**, 3077-3107.

Dudhia, J., and M. W. Moncrieff, 1989: A three-dimensionalnumerical study of an Oklahoma squall line containing right-flank supercells. *J. Atmos. Sci.*, **46**, 3363-3391.

Dudhia, J. M., and M. W. Moncrieff, 1987: Numerical simulationof quasi-stationary tropical convective bands. *Quart. J. Roy. Meteor. Soc.*, **113**, 929-967.

Dudhia, J., M. W. Moncrieff and D. W. K. So, 1987: Thetwo-dimensional dynamics of west African squall lines. *Quart. J. Roy. Meteor. Soc.*, **113**, 567-582.

Fankhauser, J. C., 1988: Estimates of thunderstorm precipitationefficiency from field measurements in CCOPE. *Mon. Wea. Rev.*, **116**, 663-684.

Ferrier, B. S., 1994: A double-moment multiple-phase four-classbulk ice scheme. Part I: Description. *J. Atmos. Sci.*, **51**, 249-280.

Ferrier, B. S., W.-K. Tao, and J. Simpson, 1995: A double-momentmultiple-phase four-class bulk ice scheme. Part II: Simulations of convective storms in differentlarge-scale environments and comparisons with other bulk parameterizations. *J. Atmos. Sci.*, **52**, 1001-1033.

Ferrier, B. S., J. Simpson and W.-K. Tao, 1996: Factorsresponsible for different precipitation efficiencies between midlatitude and tropical squall simulations. *Mon. Wea. Rev.*. **124**, 2100-2125.

Foote, G. B., and J. C. Fankhauser, 1973: Airflow and moisturebudget beneath a northeast Colorado hailstorm. *J. Appl. Meteor.*, **12**, 1330-1353.

Fovell, R. G., and Y. Ogura, 1988: Numerical simulation of amidlatitude squall line in two-dimensions. *J. Atmos. Sci.*, **45**, 3846-3879.

Fovell, R. G., and Y. Ogura, 1989: Effects of vertical wind shearon numerically simulated multicell storm structure. *J. Atmos. Sci.*, **46**, 3144-3176.

Fowler, L. D., D. A. Randall and S. A. Rutledge, 1995: Liquidand ice cloud microphysics in the CSU general circulation model. Part I: Model description andsimulated microphysical processes. *J. of Climate*, (submitted).

Frank, W. M., 1993: A hybrid parameterization with multipleclosures. *The Representation of Cumulus Convection in Numerical Models*. K. Emanuel and D. Raymond, Eds, AMS, 151-154.

Frank, W. M., and J. L. M. Bride, 1989: The vertical distributionof heating in AMEX and GATE cloud clusters. *J. Atmos. Sci.*, **46**, 3464-3478.

Fritsch, J. M., and C. F. Chappell, 1980: Numerical predictionof convectively-driven mesoscale pressure systems. Part I: Convective parameterization. *J. Atmos. Sci.*, **37**, 1722-1733.

Fritsch, J. M., R. J. Kane, and C. R. Chelius, 1986: Thecontribution of mesoscale convective weather systems to the warm-season precipitation in the United States. J. *Climate App. Meteor.*, **25**, 1333-1345.

Fu, Q., and K.-N. Liou, 1993: Parameterization of the radiativeproperties of cirrus clouds. *J. Atmos. Sci.*, **50**, 2008-2025.

Fu, Q., S. K. Krueger, and K. N. Liou, 1995: Interactions ofradiation and convection in simulated tropical cloud clusters. *J. Atmos. Sci.*, **52**, 1310-1328.

Gallus, W. A., Jr. and R. H. Johnson, 1991: Heat and moisturebudgets of an intense midlatitude squall line. *J. Atmos. Sci.*, **48**, 122-146.

Gamache, J. F., and R. A. Houze, Jr., 1983: Water budget of amesoscale convective system in the tropics. *J. Atmos. Sci.*, **40**, 1835-1850.

GEWEX Cloud System Study (GCSS), 1993: *Bull. Amer. Meteor. Soc.*, **74**, 387-400.

Grabowski, W. W., M. W. Moncrieff and J. T. Kiehl, 1997:Long-term behavior of precipitating tropical cloud systems: A numerical study. *Quart. J. Roy. Meteor. Soc.*, (in press).

Gray, W. M., and R. W. Jacobsen, 1977: Diurnal variation of deepcumulus convection. *Mon. Wea. Rev.*, **105**, 1171-1188.

Gregory, D., and M. J. Miller, 1989: A numerical study of theparameterization of deep tropical convection. *Quart. J. Roy. Mteor.*, **115**, 1209-1241.

Gregory, D., and P. R. Rountree, 1990: A mass flux correctionscheme with representation of cloud ensemble characteristics and stability-dependent closure. *Mon. Wea. Rev.*, **118**, 1483-1506.

Held, I. M., R. S. Hemler, and V. Ramaswamy, 1993:Radiative-convective equilibrium with explicit two-dimensional moist convection. *J. Atmos. Sci.*, **50**, 3909-3927.

Heymsfield, G. M., S. Schotz, 1985: Structure and evolution of asevere squall line over Oklahoma. *Mon. Wea. Rev.*, **113**, 1563-1589.

Hill, G., 1974: Factors controlling the size and spacing ofcumulus clouds as revealed by numerical experiments. *J. Atmos. Sci.*, **34**, 1934-1941.

Hill, G., 1977: Initiation mechanism and development of cumulusconvection. *J. Atmos. Sci.*, **31**, 646-673.

Houze, R. A., Jr., 1977: Structure and dynamics of a tropicalsquall-line system. *Mon. Wea. Rev.*, **105**, 1540-1567.

Houze, R. A., Jr., 1982: Cloud clusters and large-scale verticalmotions in the tropics. *J. Meteor. Soc. Japan*, **60**, 396-409.

Houze, R. A., Jr., 1989: Observed structure of mesoscaleconvective systems and implications for large-scale heating. *Quart. J. Roy. Meteor. Soc.*, **115**, 425-461.

Houze, R. A., Jr., and E. N. Rappaport, 1984: Air motions andprecipitation structure of an early summer squall line over the eastern tropical Atlantic. *J. Atmos. Sci.*, **41**, 553-574.

Johnson, R. H., 1984: Partitioning tropical heat and moisturebudgets into cumulus and mesoscale components: Implication for cumulus parameterization. *Mon. Wea. Rev.*, **112**, 1656-1665.

Johnson, R. H., and P. J. Hamilton, 1988: The relationship ofsurface pressure features to the precipitation and airflow structure of an intense mid-latitudesquall line.*Mon. Wea. Rev.*, **116**, 1444-1471.

King, M. D., L. F. Radke, and P. V. Hobbs, 1990: Determination ofthe spectral absorption of solar radiation by marine strato-cumulus clouds from airbornemeasurements within clouds. *J. Atmos. Sci.*, **47**, 894-907.

Klemp, J. B., and R. Wilhelmson, 1978: The simulation ofthree-dimensional convective storm dynamics. *J. Atmos. Sci.*, **35**, 1070-1096.

Krueger, S. K., 1988: Numerical simulation of tropical cumulusclouds and their interaction with the subcloud layer. *J. Atmos. Sci.*, **45**, 2221-2250.

Kuo, H. L., 1974: Further studies of the parameterization of theinfluence of cumulus convection on large-scale flow. *J. Atmos. Sci.*, **31**, 1232-1240.

Lafore, J.-P., and J.-L. Redelsperger, 1991: Effects of convectionon mass and momentum fields as seen from cloud-scale simulations of precipitating systems. **ECMWF Workshop on Fine-scale Modelling and the Development of Parameterization Schemes**, September 16-18, 1991, Reading, U.K., 165-197.

Lafore, J.-P., and M. W. Moncrieff, 1989: A numericalinvestigation of the organization and interaction of the convective and stratiform regions of tropicalsquall lines. *J. Atmos. Sci.*, **46**, 521-544.

Lafore, J.-P., J.-L. Redelsperger and G. Jaubert, 1988:Comparison between a three-dimensional simulation and Doppler radar data of a tropical squall line:Transport of mass, momentum, heat, and moisture. *J. Atmos. Sci.*, **45**, 3483-3500.

Lau, K. M., C. H. Sui, and W.-K. Tao, 1993: A preliminary studyof the tropical water cycle and its sensitivity to surface warming. *Bull. Amer. Meteor. Soc.*, **74**, 1313-1321.

Lau, K. M., C.-H. Sui, M.-D. Chou, and W.-K. Tao, 1994: Anenquiry into the cirrus-cloud thermostat effect for tropical sea surface temperature. *Geophys. Res. Lett.*, **21**, 1157-1160.

Leary, C. A., and R. A. Houze, Jr., 1980: The contribution ofmesocale motions to the mass and heat fluxes of an intense tropical convective system. *J. Atmos. Sci.*, **37**, 784-796.

LeMone, M. A., 1983: Momentum, transport by a line of cumulonimbus. *J. Atmos. Sci.*, **40**, 1815-1834.

LeMone, M. A., G. M. Barnes and E. J. Zipser, 1984: Momentum flux bylines of cumulonimbus over the tropical oceans. *J. Atmos. Sci.*, **41**, 1914-1932.

LeMone, M. A. and M. W. Moncrieff, 1994: Momentum and masstransport by convective bands: Comparisons of highly idealized dynamical models to observations. *J. Atmos. Sci.*, **51**, 281-305.

Li, Z., H. W. Barker, and L. Moreau, 1995: The variable effect ofclouds on atmospheric absorption of solar radiation. *Nature*, **376**, 486-490.

Lilly, D. K., 1988: Cirrus outflow dynamics. *J. Atmos. Sci.*, **45**, 1594-1605.

Lin, Y.-L., R. D. Farley, and H. D. Orville, 1983: Bulkparameterization of the snow field in a cloud model. *J. Clim.ate Appl. Meteor.*, **22**, 1065-1092.

Lindzen, R., 1990a: Some coolness concerning global warming. *Bull. Amer. Meteor. Soc.*, **71**, 288-299.

Lindzen, R., 1990b: Response to Greenhouse warming and thetropical water budget. *Bull. Amer. Meteor. Soc.*, **71**, 1465-1467.

Liou, K.-N., Q., Fu, and T. P. Ackerman, 1988: A simpleformulation of the delta-four-stream approximation for radiative transfer parameterizations. *J. Atmos. Sci.*, **45**, 1940-1947.

Lipps, F. B., and R. S. Helmer, 1986: Numerical simulation ofdeep tropical convection associated with large-scale convergence. *J. Atmos. Sci.*, **43**, 1796-1816.

Lord, S. J., 1982: Interaction of a cumulus cloud ensemble withthe large-scale environment. Part III: Semi-prognostic test of the Arakawa-Schubert cumulusparameterization. *J. Atmos. Sci.*, **39**, 88-103.

Marwitz, J. O., 1972: Precipitation efficiency of thunderstormson the High Plains. *J. Rech. Atmos.*, **6**, 367-370.

Malkus, J. S. and H. Riehl, 1964: *Cloud Structure and Distributions Over the Tropical Pacific Ocean.* University of California Press, 229 pp.

McCumber, M., W.-K. Tao, J. Simpson, R. Penc, and S.-T. Soong,1991: Comparison of ice-phase microphysical parameterization schemes using numericalsimulations of convection. *J. Appl. Meteor.*, **30**, 985-1004.

Meneghini, R., and T. Kozu, 1990: Spaceborne Weather Radar,Artech House, 197pp.

Miller, R. A., and W. M. Frank, 1993: Radiative forcing ofsimulated tropical cloud clusters. *Mon. Wea. Rev.*, **121**, 482-498.

Molinari, J., and M. Dudek, 1992: Parameterization of convectiveprecipitation in mesoscale numerical models: A critical review. *Mon. Wea. Rev.*, **120**, 326-344.

Moncrieff, M. W., 1992: Organized convective systems:Archetypal dynamical models, momentum flux theory, and parameterization. *Quart. J. Roy. Meteor. Soc.*, **118**, 819-850.

Nikajima, K., and T. Matsuno, 1988: Numerical experimentsconcerning the origin of cloud cluster in tropical atmosphere. *J. Meteor. Soc. Japan*, **66**, 309-329.

Newton, C. W., 1963: Dynamics of severe convective storms. Meteor.Monogr., 5, No. 27, 33-58.

Newton, C. W., 1966: Circulations in large sheared cumulonimbus. *Tellus*, **18**, 699-712.

Nicholls, M. E., 1987: A comparison of the results of atwo-dimensional numerical simulation of a tropical squall line with observations. *Mon. Wea. Rev.*, **115**, 3055-3077.

Nicholls, M. E, R. H. Johnson, and W. R. Cotton, 1988: Thesensitivity of two-dimensional simulations of tropical squall lines to environmental profiles. *J. Atmos. Sci.*, **45**, 3625-3649.

Nicholls, M. E, and M. J. Weissbluth, 1988: A comparison oftwo-dimensional and quasi-three-dimensional simulations of a tropical squall line. *Mon. Wea. Rev.*, **116**, 2437-2452.

Ogrua, Y., and J.-Y. Jiang, 1985: A modeling study of heating anddrying effects of convective clouds in an extratropical mesoscale system. *J. Atmos. Sci.*, 42, 2478-2492.

Pickering, K. E., J. R. Scala, A. M. Thompson, W.-K. Tao, and J.Simpson, 1992: A regional estimate of convective transport of CO from biomass burning. *Geophys. Res. Lett.*, **19**, 289-292.

Prasad, N, H.-Y. M. Yeh, R. F. Adler and W.-K. Tao, 1995:Infrared and microwave simulations of an intense convective system and comparison with aircraftobservations. *J. Appl. Meteor.*, **34**, 153-174.

Ramaswamy, V., and V. Ramanathan, 1989: Solar absorption bycirrus clouds and the maintance of the tropical upper troposphere thermal structure. *J. Atmos. Sci.*, **46**, 2293-2310.

Ramanathan, V., R. D. Cess, E. F. Harrison, P. Minnis, B. R.Barkstorm, E. Ahmad, and D. Hartmann, 1989: Radiative cloud forcing and climate: Results fromthe Earth Radiation Budget Experiment. *Science*, **121**, 985-1004.

Rotunno, R., J. B. Klemp and M. L. Weisman, 1988: A theory forstrong, long-lived squall lines. *J. Atmos. Sci.*, **45**, 463-485.

Rutledge, S.A., and P.V. Hobbs, 1984: The mesoscale andmicroscale structure and organization of clouds and precipitation in mid-latitude clouds. Part XII: Adiagnostic modeling study of precipitation development in narrow cold frontal rainbands. *J. Atmos. Sci.*, **41**, 2949-2972.

Rutledge, S. A., 1986: A diagnostic modeling study of thestratiform region associated with a tropical squall line. *J. Atmos. Sci.*, **43**, 1356-1377.

Rutledge, S. A., and R. A. Houze, Jr., 1987: A diagnosticmodeling study of the trailing stratiform rain of a mid latitude squall line. *J. Atmos. Sci.*, **44**, 2640-2656.

Scala, J. R., M. Garstang, W.-K. Tao, K. E. Pickering, A. M.Thompson, J. Simpson, V. W. J. H. Kirchoff, E. V. Browell, G. W. Saschse, A. L. Torres, G. L.Gregory, R. A. Rasmussen, and M. A. K. Khalil, 1990: Cloud draft structure and trace gas transport. *J Geophys. Res.*, **95**, 17015-17030.

Schneider, E. K., and R. S. Lindzen, 1976: A discussion of theparameterization of momentum exchange by cumulus convection. *J. Geophys. Res.*, **81**, 3158-3161.

Schlesinger, R. E., 1994: Heat, moisture and momentum budgets ofisolated deep midlatitude and tropical convective clouds as diagnosed from three-dimensionalmodel output. Part I: Control experiments. *J. Atmos. Sci.*, **51**, 3649-3673.

Simpson, J., and W.-K. Tao, 1993: The Goddard Cumulus EnsembleModel. Part II: Applications for studying cloud precipitating processes and for NASA TRMM. *Terrestrial, Atmospheric and Oceanic Sciences*, **4**, 73-116.

Simpson, J., R. F. Adler, and G. R. North, 1988: A proposedtropical rainfall measuring mission (TRMM) satellite. *Bull. Amer. Meteor. Soc.*, **69**, 278-295.

Simpson, J., C. Kummerow, W.-K. Tao, and R. Adler, 1996: On theTropical Rainfall Measuring Mission (TRMM), *Meteor. and Atmos. Phys.*, **60**, 19-36, 1996.

Simpson, J., N. E. Westcott, R. J. Clerman, and R. A. Pielke,1980: On cumulus mergers. *Arch. Meteor. Geophys. Bioklimator*, **A29**, 1-40.

Smolarkiewicz, P. K., and W. W. Grabowski, 1990: Themultidimensional positive advection transport algorithm: Nonoscillatory option. *J. Comput. Phys.*, **86**, 355-375.

Sommeria, G., 1976: Three-dimensional simulation of turbulentprocesses in an undisturbed trade wind boundary layer. *J. Atmos. Sci.*, **33**, 216-241.

Soong, S.-T., and Y. Ogura, 1980: Response of trade wind cumulito large-scale processes. *J. Atmos. Sci.*, **37**, 2035-2050.

Soong, S.-T., and W.-K. Tao, 1980: Response of deep tropicalclouds to mesoscale processes. *J. Atmos. Sci.*, **37** 2016-2036.

Soong, S.-T., and W.-K. Tao, 1984: A numerical study of thevertical transport of momentum in a tropical rainband. *J. Atmos. Sci.*, **41**,1049-1061.

Stevens, D. E., R. S. Lindzen and L. J. Shapiro, 1977: A newmodel of tropical waves incorporating momentum mixing by cumulus convection. *Dyn. Atmos. Oceans*, **1**, 365-425.

Stephens, G. L., 1978: Radiative profiles in extended waterclouds. Part II: Parameterization schemes. *J. Atmos. Sci.*, **35**, 2123-2132.

Stephens, G. L., 1984: The parameterization of radiation fornumerical weather prediction and climate models. *Mon. Wea. Rev.*, **112**, 826-867.

Stephens, G. L., and S.-C. Tsay, 1990: On the cloud absorptionanomaly. *Quart. J. Roy. Meteor. Soc.*, **116**, 671-704.

Star, D. O'C, and S. K. Cox, 1985: Cirrus clouds. Part I: A cirruscloud model. *J. Atmos. Sci.*, **42**, 2663-2681.

Sui, C. H., K. M. Lau, W.-K. Tao, and J. Simpson, 1994: Thetropical water and energy cycles in a cumulus ensemble model. Part I: Equilibrium climate. *J. Atmos. Sci.*, **51**, 711-728.

Sui, C. H., K. M. Lau, and X. Li, 1996a: Convective-radiativeinteraction in simulated diurnal variations of tropical cumulus ensemble. *J. Atmos. Sci.*, (accepted).

Sui, C. H., K. M. Lau, Y. Takayabu and D. Short, 1996b: Diurnalvariations in tropical oceanic cumulus ensemble during TOGA COARE. *J. Atmos. Sci.*, (submitted).

Tao, W.-K., 1993: A numerical study of the structure and verticaltransport properties of a tropical convective system. Ph.D. Dissertation, Department of AtmosphericScience, University of Illinois, 228 pp.

Tao, W.-K., and J. Simpson, 1984: Cloud interactions and merging:Numerical simulations. *J. Atmos. Sci.*, **41**, 2901-2917.

Tao, W.-K., and S.-T. Soong, 1986: A study of the response ofdeep tropical clouds to mesoscale processes: Three-dimensional numerical experiments. *J. Atmos. Sci.*, **43**, 2653-2676.

Tao, W.-K., and J. Simpson, 1989a: A further study of cumulusinteraction and mergers: Three-dimensional simulations with trajectory analyses. *J. Atmos. Sci.*, **46**, 2974-3004.

Tao, W.-K., and J. Simpson, 1989b: Modeling study of a tropicalsquall-type convective line. *J. Atmos. Sci.*, **46**, 177-202.

Tao, W.-K., and J. Simpson, 1993: The Goddard Cumulus EnsembleModel. Part I: Model description. *Terrestrial, Atmospheric and Oceanic Sciences*, **4**, 35-72.

Tao, W.-K., J. Simpson, and S.-T. Soong, 1991: Numericalsimulation of a sub-tropical squall line over Taiwan Strait. *Mon. Wea. Rev.*, **119**, 2699-2723.

Tao, W.-K., J. Simpson, C.-H. Sui, B. Ferrier, S. Lang, J. Scala,M.-D. Chou, and K. Pickering, 1993: Heating, moisture and water budgets of tropical and mid-latitudesquall lines: Comparisons and sensitivity to longwave radiation. *J. Atmos. Sci.*, **50**, 673-690.

Tao, W.-K., J. Scala, B. Ferrier ,and J. Simpson, 1995: Theeffects of melting processes on the development of a tropical and a mid-latitudes squall line. *J. Atmos. Sci.*, **52**, 1934-1948.

Tao, W.-K., 1995: Interaction of parameterized convection andexplicit stratiform cloud microphysics. WMO/WCRP-90, Cloud Microphysics Parameterizationsin Global Atmospheric General Circulation Models, Ed. D. Randall, 199-210.

Tao, W.-K., S. Lang, J. Simpson, C.-H. Sui and B. Ferrier andM.-D. Chou, 1996: Mechanisms of Cloud-radiation interaction in the tropics and midlatitudes. *J. Atmos. Sci.* **53**, 2624-2651.

Tripoli, G. J., and W. R. Cotton, 1989: Numerical study of anobserved orogenic mesoscale convective system. Part 2: Analysis of governing dynamics. *Mon. Wea. Rev.*, **117**, 305-328.

Warner, C., J. Simpson, G. Van Helvoirt, D. W. Martin, D.Suchman, and G. L. Austin, 1980: Deep convection on Day 261 of GATE. *Mon. Wea. Rev.*, **108**, 169-194.

Wang, Y., W.-K. Tao, and J. Simpson, 1996: The Impact of asurface layer on a TOGA COARE cloud system development. *Mon. Wea. Rev.* **124**, 2753-2763.

Webster, P. J., and G. L. Stephens, 1980: Tropical uppertroposphere extended clouds: Inferences from Winter MONEX. *J. Atmos. Sci.*, **37**, 1521-1541.

Weisman, M. L., J. B. Klemp, and R. Rotunno, 1988: Structure andevolution of numerically simulated squall lines. *J. Atmos. Sci.*, **45**, 1990-2013.

Weisman, M. L., and J. B. Klemp, 1982: The dependence ofnumerically simulated convective storms on vertical wind shear and buoyancy. *Mon. Wea. Rev.*, **110**, 504-520.

Wong, T., G. L. Stephens, P. W. Stackhouse, Jr., and F. P. J.Valero, 1993: The radiative budgets of a tropical mesoscale convective system during the EMEX-STEPExperiment. 2. Model results. *J. Geophy. Res.*, **98**, 8695-8711.

Xu, K.-M., and D. A. Randall, 1995a: Impact of interactiveradiative transfer on the microscopic behavior of cumulus ensembles. Part I: Radiationparameterization and sensitivity test. *J. Atmos. Sci.*, **52**, 785-799.

Xu, K.-M., and D. A. Randall, 1995b: Impact of interactiveradiative transfer on the microscopic behavior of cumulus ensembles. Part II: Mechanisms forcloud-radiation interactions. *J. Atmos. Sci.*, **52**, 800-817.

Xu, K.-M., and S. Krueger, 1991: Evaluation of cloudinessparameterizations using a cumulus ensemble model. *Mon. Wea. Rev.*, **119**, 342-367.

Xu, K.-M., A. Arakawa and S. Krueger, 1992: The macroscopicbehavior of cumulus ensembles simulated by a cumulus ensemble model. *J. Atmos. Sci.*, **49**, 2402-2420.

Yanai, M., S. Esbensen, and J. Chu, 1973: Determination of averagebulk properties of tropical cloud clusters from large-scale heat and moisture budgets *J. Atmos. Sci.*, **30**, 611-627.

Yau, M. K., and R. Michaud, 1982: Numerical simulation of acumulus ensemble in three dimensions. *J. Atmos. Sci.*, **39**, 1062-1079.

Yeh, H.-Y., M. N. Prasad, R. Meneghini, W.-K. Tao and R.F. Adler,1995: Model-based simulation of TRMM spaceborne radar observations. *J. Appl Meteor.*, **34**, 175-197.

Yuter, S. E., and R. A. Houze, Jr., 1995: Three-dimensionalkinematic and microphysical evolution of Florida cumulonimbus. Part II: Frequency distributions ofvertical velocity, reflectivity, and differential reflectivity. *Mon. Wea. Rev.*, **123**, 1941-1963.

Zhang, D.-A., and J. M. Fritsch, 1986: Numerical simulation ofthe meso-b scale structure and evolution of the 1977 Johnstown Flood. Part I: Modeldescription and verification. *J. Atmos. Sci.*, **43**, 1913-1943.

Zipser, E. J., 1977: Mesoscale and convective-scale downdrafts asdistinct components of squall-line structure. *Mon. Wea. Rev.*, **105**, 1568-1589.

Zipser, E. J., R. J. Meitin and M. A. LeMone, 1981: Mesoscalemotion fields associated with a slowly moving GATE convective band. *J. Atmos. Sci.*, **38**, 1725-1750.